Trapping polar molecules by surface acoustic waves

Haijin Ding [1,2] Re-Bing Wu,[3] and Yu-xi Liu [1,*]

[1]*School of Integrated Circuits, Tsinghua University, Beijing 100084, China*

[2]*Laboratoire des Signaux et Systèmes (L2S), CNRS-CentraleSupélec-Université Paris-Sud, Université Paris-Saclay, 3, Rue Joliot Curie, 91190, Gif-sur-Yvette, France*

[3]*Center for Intelligent and Networked Systems (CFINS), Department of Automation, Tsinghua University, Beijing 100084, China*

(Received 25 October 2023; accepted 26 April 2024; published 17 June 2024)

We propose a method to trap polar molecules with the electric force induced by the surface acoustic wave (SAW) on piezoelectric materials. In this approach, the electric force is perpendicular to the moving direction of the polar molecules, and is used to control the positions of trapped polar molecules in the direction orthogonal to the acoustic transmission. By virtue of an external electric force, the SAW-induced electric field can trap the polar molecules into single-layer or multilayer lattices. The arrangement of molecules can affect the binding energy and localization of the molecule array. Then the one- or two-dimensional trapped polar molecule arrays can be used to construct the Bose-Hubbard (BH) model, whose energy and dynamics are affected by the localizations of the trapped molecules. We find that the phase transitions between the superfluid and Mott insulator based on trapped polar molecule BH model can be modulated by the SAW-induced electric potential.

DOI: 10.1103/PhysRevResearch.6.023292

I. INTRODUCTION

Polar molecules have many potential applications such as in quantum computation [1–6] and simulations [7–10]. The first step towards manipulating polar molecules is to decelerate and trap them for further operations [11]. It has been shown that polar molecules can be trapped by magnetic [12–14], optical [15–19], or electric fields [19–25]. For examples, in the magneto-electrostatic trap, polar molecules can be stably trapped by the magnetic quadrupole after deceleration [13]. By additionally applying both dc and ac electric fields, the molecules can also be trapped through mechanical equilibrium [24,26,27]. Once successfully trapped, the internal rovibronic state, center of mass, and interactions among different polar molecules can be further modulated via additional control fields [28–30]. Variational efficient trapping approaches allow for more possible applications by controlling the trapped molecules [7,31].

The interaction between electric fields and polar molecules can be examined via the Stark effect, where the electric field modulates the spectral properties of polar molecules [32–35]. Based on this, polar molecules can be controlled or rotated by an electric field because of asymmetric structure and larger dipole moments, and this is different from the behavior of neutral atoms [5]. The doublet splitting of polar molecules induced by the electric field can affect the Stark potential, which can further determine the mechanical potential, mechanical force, and mechanical motions of polar molecules [36–39].

Surface acoustic wave (SAW) devices have been extensively applied to classical information processing [40,41]. The SAW, a kind of mechanical wave within the piezoelectric materials, is excited by an external ac voltage source upon the interdigital transducers (IDTs), which can transform the electrical energy to the mechanical energy in the form of propagating acoustic wave on the surface of the piezoelectric substrate or reversely transform the acoustic wave to the electrical energy. The induced electric potential by SAW can drive electrons to generate zero-resistance states [42], acousto-electrical currents [43], and metal-Mott insulator phase transitions [44]. With the tunable external ac source, the SAW in the piezoelectric materials can provide a well-controlled time-dependent moving electric potential, and can be designed to control electronic [45] or polar particles [43,46].

In this paper, we propose a method to trap polar molecules using the electric field in the free space carried by the SAW propagating along the surface of the piezoelectric substrate materials. To trap and control the polar molecule by the electric force via its dipole moment [5,47,48], we consider that the surface acoustic wave can induce electric potential both in the piezoelectric material and in the free space over electrodes [45,49–51]. This is similar to the situation where polar molecules can be modulated by the electric forces applied by the electrodes with periodic voltages [20,52].

The remainder of this paper is organized as follows. In Sec. II, we explore the possibility that polar molecules are trapped as one-, two-, and three-dimensional arrays by the electric field induced by IDTs of SAW combined with another externally applied electric force. In Sec. III, we study how the trapping approach can affect the property of the multilayer trapped polar molecules. In Sec. IV, we clarify the spatial dis-

*yuxiliu@mail.tsinghua.edu.cn

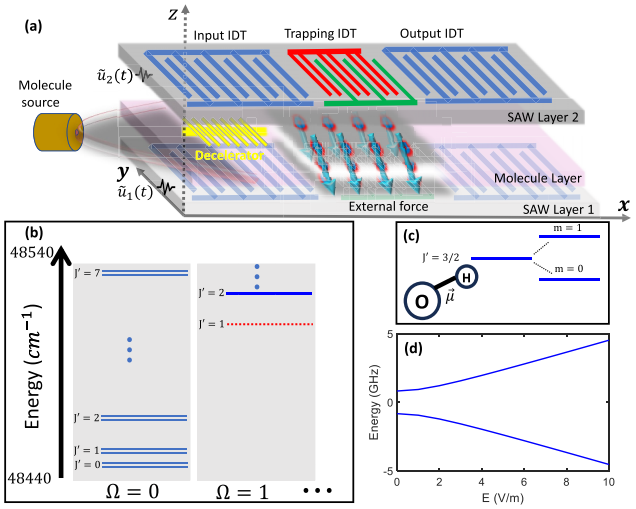

FIG. 1. (a) Schematic diagram for a setup of trapping polar molecules with SAW-induced fields and the external electric force. (b) The energy level structure of CO with different quantum numbers [20,52]. (c) The energy level structure of OH molecule with a stronger polarity [34]. (d) The energy level structure of OH molecule affected by the electric field when $E_\Lambda = 1.65$ GHz, $|\vec{\mu}| = 1.67$ Debye valued by Debye length, $J' = 3/2$ and $m = \Omega = 1$ [34].

tribution of the single-layer trapped molecules. In Sec. V, we study the dynamics and phase transition of the Bose-Hubbard model based on polar molecules, which are trapped in lattices by SAW. Finally, conclusions are presented in Sec. VI.

II. THEORETICAL MODEL FOR TRAPPING POLAR MOLECULES

As schematically shown in Fig. 1(a), polar molecules transmit between two layers of piezoelectric materials after being slowed down by a decelerator. In each piezoelectric layer, both the input and output IDTs consist of two comb-shaped arrays of metallic electrodes [i.e., the blue electrodes in the two SAW layers in Fig. 1(a)]. The primary functions of IDTs are to convert electric signals to SAW, or convert SAW back to the electrical signal via piezoelectric effect. Driven by the external electric fields $\tilde{u}_1(t)$ and $\tilde{u}_2(t)$, the input IDT excites acoustic waves and the output IDT converts SAW into electrical signals. In the middle trapping IDT, the three electrodes [i.e., two red electrodes and one green electrode in the upper layer of Fig. 1(a)] in each unit can transfer the mechanical oscillation of the SAW to the electric field in the open space, during which the propagation of the acoustic wave remains unaffected by canceling out the reflection waves in the piezoelectric material [40,53]. Besides electric field from the trapping IDT, externally designed electric fields, represented with the blue down arrows in Fig. 1(a), can also be applied to the space between two layers of SAWs. The external electric fields can be realized and modulated by a three-dimensional electrode array as in Ref. [54] or Appendix A 3. Additionally, to enhance the efficiency of interactions, the two piezoelectric layers face each other with the electrodes exposed to the open space between them. This set up allows the energy of polar molecules, i.e., CO with the energy structure as in Fig. 1(b) or hydroxyl radical (OH) as in Fig. 1(c), to be affected by the electric field generated by SAW as follows.

A. Interaction between polar molecules and the electric field by SAW

According to the calculations shown in Appendix A, in the free space between two piezoelectric layers, the electric field converted by the trapping IDT in the middle part of each layer can be represented as

$$\begin{aligned} E_x^{(j)}(x,z,t) &= M\bar{u}_j k e^{-k\tilde{z}_j}\sin\left[k\left(x-\tfrac{2\lambda}{3}-vt\right)\right],\\ E_z^{(j)}(x,z,t) &= (-1)^{j-1}M\bar{u}_j k e^{-k\tilde{z}_j}\cos\left[k\left(x-\tfrac{2\lambda}{3}-vt\right)\right], \end{aligned} \tag{1}$$

where $j = 1, 2$ represent the electric fields induced by the lower and upper SAW layer respectively, x represents the propagation direction of the acoustic wave, z represents the vertical direction to the surface distinguished by $(-1)^{j-1}$ for the positive and negative directions, M is the number of units for the trapping IDT [i.e., $M = 3$ in Fig. 1(a)], $\bar{u}_j$ is the amplitude of the voltage between the red and green electrodes of the trapping IDT, λ is the wavelength of the acoustic wave that is equal to the periodicity of IDT stripes [53], $\tilde{z}_j$ is the distance to the lower or upper SAW layer with $\tilde{z}_1 = z$ and $\tilde{z}_2 = D - z$ where D is the distance between two layers of piezoelectric materials, v is the velocity of the acoustic wave, and k is the wave number. More details on the architecture design, the realization of external electric force represented by the down arrows in Fig. 1(a), and the solutions of the acoustic waves are given in Appendix A.

When there is no external electric force applied to the polar molecule, the molecular dynamics is governed by the Hamiltonian $H_0 = B\mathbf{J}^2$, where $\mathbf{J}$ is the rotational angular momentum and B is the rotational constant [55]. When the polar molecules are over the IDT array of the surface acoustic wave, the electric field induced by the SAW in the jth layer can be coupled to the polar molecule via electric dipole interactions, described by the Hamiltonian as [7,55]

$$H_I = -\vec{\mu}\cdot\vec{E}^{(j)}(x,z,t), \tag{2}$$

where $\vec{\mu}$ is the dipole moment of the polar molecule, and the field $\vec{E}^{(j)}(x,z,t) = [E_x^{(j)}(x,z,t), E_z^{(j)}(x,z,t)]^T$ given in Eq. (1) is from the trapping IDTs (for more details see Appendix A). When the electric field by SAW is weak, the polar molecules {i.e., OH in Ref. [34], KCs in Ref. [3], CaBr in Ref. [5], deuterated ammonia (ND_3) in Ref. [23], CO in Refs. [6,20,52]} can be regarded as a two-state system. The electric field along different directions has different coupling strengths with the dipole moments even for a given quantum number [36]. Here we consider the case in which the dipole moments of polar molecules are along the z direction, then Eq. (2) is further written as [20,36,52,56]

$$H = \begin{bmatrix} \omega_2 & -|\vec{\mu}|E_z^{(j)}(x,z,t)\frac{m\Omega}{J'(J'+1)} \\ -|\vec{\mu}|E_z^{(j)}(x,z,t)\frac{m\Omega}{J'(J'+1)} & \omega_1 \end{bmatrix}, \tag{3}$$

where we consider two energy levels of the polar molecule as $\hbar\omega_l$ with $l = 1, 2$, $\omega_2 - \omega_1 = \bar{E}_\Lambda$ is the Λ-doublet splitting; $E_z^{(j)}(x,z,t)$ is given in Eq. (1); J', Ω, and m are the quantum

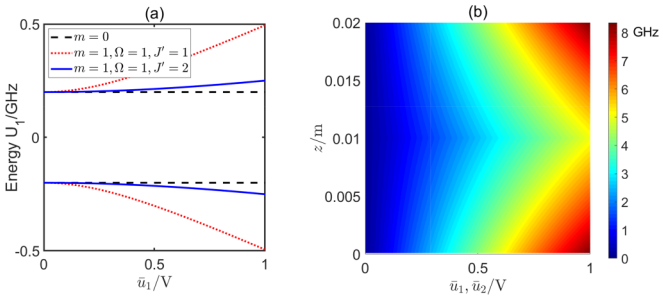

FIG. 2. (a) The dependence of the energy levels of polar molecules on the electric field with different quantum numbers, where the distance between the molecules and the lower SAW layer is $z = 0.01$ m, $E_\Lambda = 0.4$ GHz, $|\vec{\mu}| = 0.167$ Debye and the wave number $k = 10$. (b) The energy level of polar molecules CO evaluated by $\max(U_j(\bar{u}_j, z))$ with $j = 1, 2$ representing the lower or upper SAW when $k = 50$, $E_\Lambda = 0.4$ GHz, $|\vec{\mu}| = 0.167$ Debye, $J' = m = \Omega = 1$ [36].

numbers according to the energy level structure of a polar molecule, i.e., J' is the index of the energy level, Ω and m with the values $-1, 0, 1$ represent quantum numbers for the basis state of the molecule wave function [36].

In the rotating reference frame (RRF) with the rotating wave approximation (RWA) [57,58], the Hamiltonian representing the interaction between the polar molecule and electric field can be simplified as

$$H' = \begin{bmatrix} \bar{\omega} + \frac{\bar{E}_\Lambda - kv}{2} & (-1)^j \frac{|\vec{\mu}|m\Omega}{2J'(J'+1)} \mathcal{E}_x^* \bar{E}_z^{(j)} \\ (-1)^j \frac{|\vec{\mu}|m\Omega}{2J'(J'+1)} \mathcal{E}_x \bar{E}_z^{(j)} & \bar{\omega} - \frac{\bar{E}_\Lambda - kv}{2} \end{bmatrix}, \quad (4)$$

where $\bar{E}_z^{(j)} = M\bar{u}_j k e^{-k\tilde{z}_j}$, $\mathcal{E}_x = e^{-ik(x-\frac{2\lambda}{3})}$, $\bar{\omega} = (\omega_1 + \omega_2)/2$ (more details are given in Appendix B). Then the energy levels of the polar molecule affected by the electric field produced by the SAW in the jth layer are

$$\begin{aligned} \mathbf{E}_j &= \bar{\omega} \pm \sqrt{\left(\frac{E_\Lambda}{2}\right)^2 + \mu_{\text{eff}}^2 M^2 \bar{u}_j^2 k^2 e^{-2k\tilde{z}_j}} \\ &\equiv \bar{\omega} + U_j, \end{aligned} \quad (5)$$

where $E_\Lambda = \bar{E}_\Lambda - kv$, $U_j = \pm\sqrt{(E_\Lambda/2)^2 + \mu_{\text{eff}}^2 |\bar{E}_z^{(j)}|^2}$ representing the modulation of energy levels by the SAW provided electric field, the effective dipole strength $\mu_{\text{eff}} = \pm|\vec{\mu}|m\Omega/2J'(J'+1)$, which can be positive for the high-field seeking states or negative for the low-field seeking states [36,59]. Obviously, $\mathbf{E}_j$ is independent of $\mathcal{E}_x$ in the RRF. In the following, we take $M = 1$ for simplification.

The energy levels of the polar molecule in Fig. 1(d) are with the parameters in Ref. [34] and in Fig. 2 with the parameters in Refs. [20,36,52], which are affected by the electric field along the z direction. We find that the energy gap strongly depends on the quantum number and the amplitude of voltage.

B. Trapping polar molecules into one-, two-, and three-dimensional lattices

If we want to trap the polar molecule at $\vec{r} = [x_0, z_0]$, the joint electric force applied to the polar molecule $\vec{F}(x_0, z_0, t)$ must satisfy the following conditions [25,60,61]:

$$\begin{aligned} \vec{F}(x_0, z_0, t) &\equiv 0, \\ \vec{\nabla} \cdot \vec{F}(x_0, z_0, t) &< 0, \end{aligned} \quad (6)$$

where the first line is for the mechanical equilibrium, and the second line represents the occurrence of resilience effect once the molecules escape from the trapped site (x_0, z_0).

As a component of $\vec{F}(x_0, z_0, t)$, the electric force from the trapping IDT of the jth SAW layer can be represented as $\vec{F}^{(j)}(x, z, t) = [F_x^{(j)}(x, z, t), F_z^{(j)}(x, z, t)]^T$ when the molecule moves slowly along the x direction after deceleration, and $\vec{F}^{(j)}(x, z, t)$ is determined by the strength of the electric field from the trapping IDTs and the quantum number of the polar molecule. With the energy U_j in Eq. (5), the electric force produced by SAW upon polar molecules reads [20]

$$\begin{aligned} \vec{F}^{(j)}(x, z, t) &= -\frac{dU_j}{d|\bar{E}_z^{(j)}|} \vec{\nabla} |\bar{E}_z^{(j)}| \\ &= -\frac{1}{2} \frac{1}{|\bar{E}_z^{(j)}|} \frac{dU_j}{d|\bar{E}_z^{(j)}|} \vec{\nabla} |\bar{E}_z^{(j)}|^2, \end{aligned} \quad (7)$$

where

$$dU_j/d|\bar{E}_z^{(j)}| = \mu_{\text{eff}}^2 |\bar{E}_z^{(j)}| / \sqrt{(E_\Lambda/2)^2 + \left(\mu_{\text{eff}} |\bar{E}_z^{(j)}|\right)^2},$$

then

$$F_x^{(j)}(x, z, t) = 0, \quad (8a)$$

$$F_z^{(j)}(x, z, t) = \frac{\mu_{\text{eff}}^2 \bar{u}_j^2 k^3 e^{-2k\tilde{z}_j}}{\sqrt{\left(\frac{E_\Lambda}{2}\right)^2 + \left(\mu_{\text{eff}} |\bar{E}_z^{(j)}|\right)^2}}. \quad (8b)$$

Additionally, we can also have

$$\vec{\nabla} \cdot \vec{F}^{(j)}(x, z, t) = -\frac{\mu_{\text{eff}}^2 \left[\left(\frac{\partial^2 \phi}{\partial x^2}\right)^2 + \left(\frac{\partial^2 \phi}{\partial z^2}\right)^2 + 2\left(\frac{\partial^2 \phi}{\partial z \partial x}\right)^2\right]}{\sqrt{\left(\frac{E_\Lambda}{2}\right)^2 + \left(\mu_{\text{eff}} |\vec{E}^{(j)}|\right)^2}} < 0, \quad (9)$$

where $\phi = \phi_j(x, z)$ is the electric potential produced by trapping IDTs in the jth SAW layer (more details are given in Appendix C). Equation (9) indicates that the electric field induced by SAW can trap the polar molecules if the condition of the equilibrium in Eq. (6) can be satisfied.

When $\bar{u}_1$ and $\bar{u}_2$ are nonzero and there are no external forces, the polar molecules can be trapped by the electric forces of IDTs between two piezoelectric materials, and the trapped location z_0 of molecules is determined by the equilibrium with $\bar{u}_1^2 e^{-2kz_0} = \bar{u}_2^2 e^{-2k(D-z_0)}$, where $\bar{u}_1$ and $\bar{u}_2$ are proportional to the amplitudes of $u_1(t)$ and $u_2(t)$ in Fig. 1(a), respectively. Then we can obtain the trapping location $z_0 = \ln(e^{kD}\bar{u}_1/\bar{u}_2)/2k$, the relationship $e^{-kD} < \bar{u}_1/\bar{u}_2 < e^{kD}$ always holds because $0 < z_0 < D$, and this agrees with the fact that larger D induces more robust parameter settings of $\bar{u}_1$ and $\bar{u}_2$ for trapping the molecules. As shown in Fig. 3(a), the trapping locations are closer to the lower SAW layer when $\bar{u}_1 > \bar{u}_2$ and are closer to the upper SAW layer when $\bar{u}_2 > \bar{u}_1$. In this way, a single layer of polar molecules can be trapped at arbitrary locations of the height z_0. Besides, here the potential applied on the polar molecules is the joint potential generated by the trapping IDTs of the upper and lower SAW layers. Then

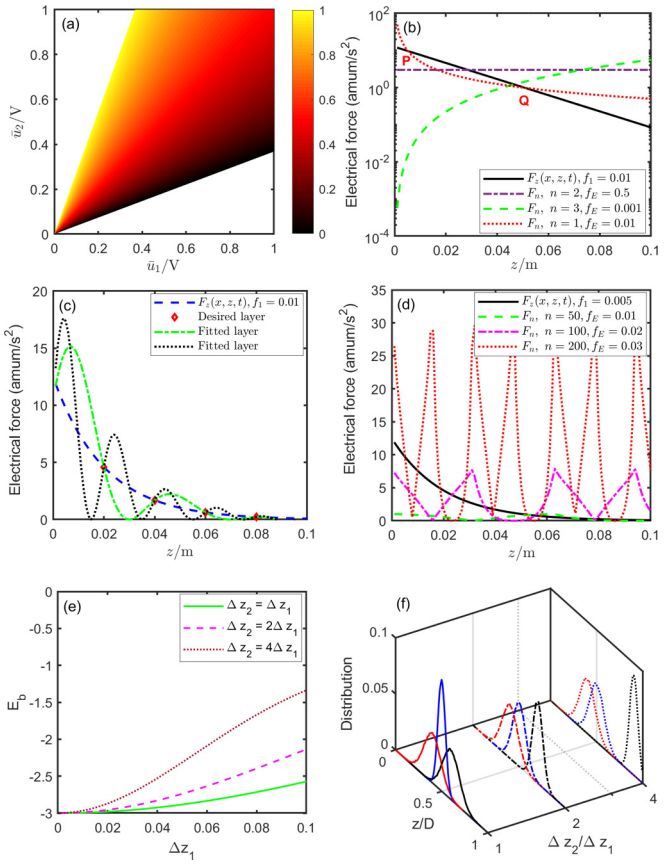

FIG. 3. (a) Trapping locations with two layers of surface acoustic waves, where $k = 50$, $D = 0.02$ m, and z_0/D are evaluated. The blank area represents that the molecules cannot be trapped for values of $\bar{u}_1$ and $\bar{u}_2$. (b) $F_z(x, z, t)$ represents the force of the lower SAW with different locations of z, the dashed or dotted curves represent the force of different external electric fields represented as $\tilde{E}(z) = f_E z^n$. The electric forces are valued by the unit amu m/s^2 as in Ref. [54] with amu representing the atomic mass unit [62]. When the dashed curve and the solid curve intersect once, it means that the molecules can be only trapped in the single layer with the value of z at the crossover point. When the dotted curve and the solid curve intersect twice as the red curve, the polar molecules can be trapped in two layers at the two crossover points. (c) Green-dashed curve represents the electric field $\tilde{E}(z) = (-2.42 \times 10^4 z^3 + 5201z^2 - 389.6z + 10.5)(1 + \sin(\pi z/0.02))$ with an envelope of a sine function to trap within the desired layers, and the trapping by the black-dotted curve with a cosine envelop is more stable because the joint force has different restoring directions below or over the desired layers. (d) Nonuniform trapping of polar molecules with the external electric field $\tilde{E}(z) = f_E \sin(nz)$ with different values of n and f_E, and the force upon the polar molecule reads $F_n = |nf_E^2 \sin(nz)\cos(nz)/(|f_E \sin nz| + \tilde{\epsilon})|$ where we take $\tilde{\epsilon} = \sqrt{(E_\Lambda/2/\mu_{\text{eff}})^2 + |\tilde{E}(z)|^2} - |\tilde{E}(z)| \approx 0.01$ and is close to zero [36]. (e) Comparison of the binding energy with different trapped locations of layers with $\alpha = 8$. (f) The distribution of trapped locations of polar molecules along the z direction in different layers, which can be valuated with R_j in Eq. (14) with $R_0 = 0.04$, $\xi = 0.01\text{m}^2$, $z_2 = 0.5D$, and $\Delta z_2 = 0.4D$. The parameters in (e) and (f) are chosen according to Refs. [62,63].

Eq. (C1) in Appendix C reveals that the molecules can be stably trapped at the equilibrium positions.

When $\bar{u}_1 \neq 0$ and $\bar{u}_2 = 0$, the polar molecules can be trapped at (x_0, z_0) by the electric field induced by the trapping IDT in the lower SAW layer and the external electric force $\tilde{F}_z(x_0, z_0, t)$, which satisfies the equilibrium condition, that is

$$\begin{aligned}\tilde{F}_z(x_0, z_0, t) &= F_z^{(1)}(x_0, z_0, t) \\ &= \frac{\mu_{\text{eff}}^2 M^2 \bar{u}_1^2 k^3 e^{-2kz_0}}{\sqrt{(E_\Lambda/2)^2 + \left(\mu_{\text{eff}} \left|\bar{E}_z^{(1)}\right|\right)^2}} \\ &\triangleq f_1 k^2 e^{-kz_0},\end{aligned} \tag{10}$$

with $f_1 \approx \mu_{\text{eff}} M \bar{u}_1$. $\tilde{F}_z(x_0, z_0, t)$ can be used to cancel $F_z^{(1)}(x_0, z_0, t)$ based on the approximation $E_\Lambda \ll |\bar{E}^{(1)}(x, z, t)|$ [46].

The external electric force $\tilde{F}_z(x_0, z_0, t)$ can be realized with the external electric field $\tilde{E}(z)$ applied upon the polar molecule array, then the mechanical equilibrium along z direction can be realized when [36]

$$\frac{1}{2|\tilde{E}(z)|} \frac{\partial |\tilde{E}(z)|^2}{\partial z} = f_1 k^2 e^{-kz}, \tag{11}$$

by representing $\tilde{F}_z(x_0, z_0, t)$ in Eq. (10) with the format of $\tilde{E}(z)$, and the equation is independent of x. Mathematically, different $\tilde{E}(z)$ can induce different trapping results for polar molecules. For example, when $D = 10$ cm and $k = 50$, various trapping approaches are compared in Figs. 3(b)–3(d).

Unlike trapping with two SAW layers, where the molecules can be trapped at arbitrary horizontal locations at z_0 with an unlimited number of trapped molecules, the polar molecules can only be trapped at the location where an external force for the equilibrium exists, as shown in Fig. 1(a) when only one SAW layer is used for trapping. Then the molecules can be trapped in a lattice with external electric force at the height z determined by the one or several different intersections as shown in Figs. 3(b)–3(d).

Further for the simulations in Fig. 3(b), the red curve denoting external electric force has two intersection points P and Q with the SAW-induced electric force. For the lower intersection point P at the height z_p, the combined force is downward when $z < z_p$ and upward when $z > z_p$, thus the trapped polar molecules can easily escape from the trapped site at z_p. However, for the upper intersection point Q at the height z_q, the combined force is upward when $z < z_q$ and downward when $z > z_q$, and this provides a resilience along the z direction to make sure that the polar molecules are stably trapped at z_q. This is why in Fig. 3(c), the black-dotted curve can trap the polar molecules at the desired layers more stably than the green-dashed curve. Although the black-dotted curve can simultaneously introduce unstable trapped intersections, while the number of trapped polar molecules is much less than that by the stable intersections.

Once the polar molecules are stably trapped by the electric force, the interactions among molecules are affected by

their locations and external electric potentials. In the following, we discuss three different cases: The first is that the polar molecules are trapped as a three-dimensional array, where the lattice sites in each layer are remotely separated in the horizontal direction and the horizontal hoppings are not considered. The second case is that a single layer of polar molecules is trapped and the horizontal hoppings are considered. The third case is that the polar molecules are trapped by one SAW layer (i.e., the upper layer) and the external force in lattices, but their quantum dynamics are also affected by the electric potential induced by the other SAW layer, so that the lattice dynamics can be influenced by the lower SAW.

III. THREE-DIMENSIONAL TRAPPED POLAR MOLECULE ARRAY WITH MULTIPLE LAYERS

When the polar molecules with a three-dimensional structure are trapped at different heights, as schematically shown in Fig. 1(a), the number of trapped molecules in each layer is the same. This is because the external electric forces F_n are applied along the z direction across each molecule layer, where F_n is similarly calculated as $\vec{F}^{(j)}(x, z, t)$ in Eq. (7) by replacing $\tilde{E}_z^{(j)}$ with $\tilde{E}(z)$ under the approximation $E_\Lambda \ll \max|\tilde{E}(z)|$. For example, in Fig. 3(b) when $n = 3$ and $f_E = 0.001$, the polar molecules can be trapped in a single layer that corresponds to the intersection point between the black and green curves. By multiplying $\tilde{E}(z)$ with an envelope function, i.e., $f_{ev} = 1 + \prod_{j=1}^{N}(z - z_j)$ or $f_{ev} = 1 + \sin(\pi z/\Delta_z)$ with $\Delta_z = 0.02$ as shown in Fig. 3(c), the polar molecules can be evenly (green dash) or not evenly [Fig. 3(d)] trapped at the designed heights with $z_1, z_2, \cdots, z_N$. The method can also be generalized to the case of $\bar{u}_1 = 0$ and $\bar{u}_2 \neq 0$, representing that molecules can be trapped with the upper SAW layer and the external electric field.

When the polar molecules are trapped as a three-dimensional array, the attractive interactions among molecules in different trapped layers can bind them into chains along z direction, and the molecular attraction can be evaluated with the binding energy depending on the number and height of trapped layers. The Hamiltonian of the trapped polar molecules along z direction reads [62]

$$H_L = \sum_{l=1}^{L}\left(\frac{P_l^2}{2m_0} + \frac{m_0\omega^2 r_l^2}{2}\right) + \frac{1}{2}\sum_{q\neq l}^{L} V_{|q-l|}(|z_i - z_l|), \quad (12)$$

where m_0 is the mass of the trapped polar molecules in each layer, L is the number of trapped layers, P_l and r_l are the momentum and the position of the center-of-mass of the molecules in the lth layer, respectively, $\omega \propto k$ is the trapping frequency of the molecules, and $V_{|q-l|}$ is the dipole-dipole interaction between molecules in the qth and lth layers determined by the trapped height z_q and z_l respectively. The variational wave function of the L layers of trapped polar molecules is [62]

$$\psi_L(r_1, \cdots, r_L) = \prod_{l=1}^{L}\frac{\exp\left(-|r_l|^2/2R_l^2\right)}{\sqrt{\pi}R_l}, \quad (13)$$

where the standard deviation R_l of the normal distribution is determined by the equilibrium of the attractive forces between the polar molecules in the layers on its upper and lower sides. When the molecules are uniformly trapped along the z direction, as in Ref. [62], R_l is the smallest at the middle layer. However, when the polar molecules are not uniformly trapped, R_l should be proportional to $1 + \xi|F_\uparrow^l - F_\downarrow^l|$ where $F_\uparrow^l = \sum_{q=l+1}^{L} \mathrm{d}V_{|q-l|}/\mathrm{d}|z_q - z_l|$ is the attractive force by the upper trapped polar molecules, $F_\downarrow^l = \sum_{q=1}^{l-1} \mathrm{d}V_{|q-l|}/\mathrm{d}|z_q - z_l|$ is the attractive force by the lower trapped polar molecules, and ξ is a chosen parameter. Then, we have

$$R_l = R_0\left(1 + \xi\left|\sum_{q=l+1}^{L}\frac{1}{|z_q - z_l|^2} - \sum_{q=1}^{l-1}\frac{1}{|z_q - z_l|^2}\right|\right) \quad (14)$$

as a generalization of the formula in Ref. [62], and the parameter R_l is determined by the trapped locations of different polar molecule layers. For the multilayer trapped molecules, the binding energy representing the required energy to separate the layers reads $E_b = \sum_{q\neq l} E_b^{ql} \approx -\sum_{q\neq l}\exp(-\alpha(z_q - z_l)^2)$ [63].

Consider the case where three molecules layers are trapped at the heights $z_1 < z_2 < z_3$ as an example. Denote $\Delta z_1 = z_2 - z_1$ and $\Delta z_2 = z_3 - z_2$. The comparisons of the binding energy and the oscillations of polar molecules in different layers are shown in Figs. 3(e) and 3(f) with the parameters chosen according to Ref. [62]. The absolute value of the binding energy for the multilayer polar molecule array is larger when the molecules are closely trapped along the z direction. When the layers are uniformly trapped with $\Delta z_1 = \Delta z_2$, the oscillation of the center layer is reduced. However, when the layers are nonuniformly trapped in dispersed locations, the oscillation of polar molecules is stronger due to the unequalizing of the attractive force along the z direction. Besides, the distributions of polar molecules in different layers are influenced by the thermal effect, as discussed in detail in Ref. [62].

IV. SPATIAL DISTRIBUTION OF TRAPPED MOLECULES

In a single trapped polar molecule layer, the polar molecules can hop among different localized lattice sites via quantum jumps, which can be called the Anderson localization [64,65]. When the molecules are trapped by the lower SAW as shown in Fig. 1(a) and an external electric field as shown in Figs. 3(b)–3(d), the molecules can be further trapped in 1D or 2D lattices, and the locations of the lattices are determined by the spatial distribution of the external electric fields in the plane orthogonal to the z axis. We denote the probability amplitude as $p_{\mathbf{n}}$ that a molecule is trapped at the lattice labeled with $\mathbf{n}$, where $\mathbf{n} = n$ when the molecules are trapped in a 1D lattice and $\mathbf{n} = (n_x, n_y)$ for a 2D lattice. We use the one-dimensional trapped polar molecules along the x axis as an example, the external electric field for trapping is imposed at $x_1, x_2, \cdots, x_N$, the evolution of p_n reads [64]

$$\dot{p}_n(t) = -iU_0 p_n(t) - i\sum_{j\neq n} v_{nj} p_j(t), \quad (15)$$

where U_0 is the energy of the polar molecules, $v_{nj} \propto |x_n - x_j|^{-3}$ represents the dipole interaction between the polar molecules trapped at the nth and jth lattices, and $1 \leqslant n, j \leqslant N$.

Applying the Laplace transform to Eq. (15), we have

$$P_n(s) = \frac{p_n(0) - i\sum_{j\neq n} v_{nj}P_j(s)}{s + iU_0} = \frac{ip_n(0)}{is - U_0} + \sum_{j\neq n}\frac{1}{is - U_0}v_{nj}P_j(s), \tag{16}$$

where $P_j(s)$ is the Laplace transformation of $p_j(t)$.

Let us assume initially that $p_1(0) = 1$ and $p_n(0) = 0$ for $n = 2, 3, \cdots, N$, that is, only molecules at the first lattice are initially trapped. Equation (16) with $n = 1$ reads [64]

$$P_1(s) = \frac{i}{is - U_0} + \sum_{j=2}^{N}\frac{1}{is - U_0}v_{1j}P_j(s), \tag{17}$$

and

$$P_n(s) = \sum_{j\neq n}\frac{1}{is - U_0}v_{nj}P_j(s) = \frac{1}{is - U_0}v_{n1}P_1(s) + \sum_{j=2}^{n-1}\frac{1}{is - U_0}v_{nj}P_j(s) + \sum_{n+1}^{N}\frac{1}{is - U_0}v_{nj}P_j(s), \tag{18}$$

for $n = 2, 3, \cdots, N$.

Using Eq. (18), Eq. (17) becomes

$$\begin{aligned} P_1(s) &= \frac{i}{is - U_0} + \sum_{j=2}^{N}\frac{1}{is - U_0}v_{1j}\left[\frac{1}{is - U_0}v_{j1}P_1(s) + \sum_{j'=2}^{j-1}\frac{1}{is - U_0}v_{jj'}P_{j'}(s) + \sum_{j+1}^{N}\frac{1}{is - U_0}v_{jj'}P_{j'}(s)\right] \\ &= \frac{i}{is - U_0} + \frac{P_1(s)}{(is - U_0)^2}\sum_{j=2}^{N}v_{1j}^2 + \frac{1}{(is - U_0)^2}\sum_{j=2}^{N}v_{1j}\left[\sum_{j'=2}^{j-1}v_{jj'}P_{j'}(s) + \sum_{j+1}^{N}v_{jj'}P_{j'}(s)\right] \\ &\approx \frac{i}{is - U_0} + \frac{P_1(s)}{(is - U_0)^2}\sum_{j=2}^{N}v_{1j}^2 + \frac{1}{(is - U_0)^3}\sum_{j=2}^{N}v_{1j}\left[\sum_{j'=2}^{j-1}v_{jj'}v_{j'1}P_1(s) + \sum_{j+1}^{N}v_{jj'}v_{j'1}P_1(s)\right], \end{aligned} \tag{19}$$

where $P_{j'}(s) \approx \frac{1}{is - U_0}v_{j'1}P_1(s)$ has been used. Then

$$P_1(s) \approx \frac{i}{is - U_0} + \frac{\sum_{j=2}^{N}v_{1j}^2}{(is - U_0)^2}P_1(s) + \frac{1}{(is - U_0)^3}\sum_{j=2}^{N}v_{1j}\left(\sum_{j'=2}^{j-1}v_{jj'}v_{j'1} + \sum_{j+1}^{N}v_{jj'}v_{j'1}\right)P_1(s). \tag{20}$$

Denoting $\alpha = \sum_{j=2}^{N}v_{1j}^2$ and $\beta = \sum_{j=2}^{N}v_{1j}\left(\sum_{j'=2}^{j-1}v_{jj'}v_{j'1} + \sum_{j+1}^{N}v_{jj'}v_{j'1}\right)$, then we have

$$P_1(s) = \frac{i(is - U_0)^2}{(is - U_0)^3 - \alpha(is - U_0) - \beta} = \frac{i(is - U_0)^2}{-is^3 + 3U_0s^2 + i\left(3U_0^2 - \alpha\right)s - U_0^3 + \alpha U_0 - \beta}. \tag{21}$$

For most of the case $U_0^3 - \alpha U_0 + \beta \neq 0$, thus $\lim_{t\to\infty}p_1(t) = \lim_{s\to 0}sP_1(s) = 0$.

The trapped molecule array in Fig. 3(a) can be regarded as a lattice network with infinite number of sites and the spatial distribution of trapped localizations converges with the increase of N, as shown in Figs. 4(a) and 4(b).

A. Comparison of diffusion based on the single-layer trapped polar molecules

Generalized from the case in Eq. (15), when the polar molecules are trapped by two SAW layers as shown in Fig. 1(a) without the external electric force, the molecules can be trapped at arbitrary locations along the x direction, the spatial distribution of the molecules is governed by

$$\dot{p}_x(x,t) = -iU_0p_x(x,t) - i\int_0^{x_-}v_{xx'}p_{x'}(x',t)\mathrm{d}x' - i\int_{x_+}^{M\lambda}v_{xx'}p_{x'}(x',t)\mathrm{d}x', \tag{22}$$

where $p_x(x,t)$ and $p_{x'}(x',t)$ are the probability amplitudes of the trapped molecules at x and x', respectively; $v_{xx'} \propto |x - x'|^{-3}$ represents the interaction between the sites at x and x'; the parameters M and λ are the same as that in Eq. (1).

The continuous model in Eq. (22) can be approximated by the discrete model in Eq. (15) when $N \to \infty$ and $\Delta x = x_n - x_{n-1} \approx 0$ for $n = 2, 3, \cdots, N$. Then by Eqs. (20) and (21), considering that the condition $U_0^3 - \alpha U_0 + \beta = 0$ can almost never be satisfied, we have $\lim_{t\to\infty}p_1(t) = \lim_{s\to 0}sP_1(s) = 0$. This agrees with the case in Fig. 4(a) when $N = 500$.

B. Cooperative shielding

Together with the long range interactions, the evolution of the quantum states $|\psi(t)\rangle = \sum_{n=1}^{N}c_n(t)|n\rangle$ is governed by the

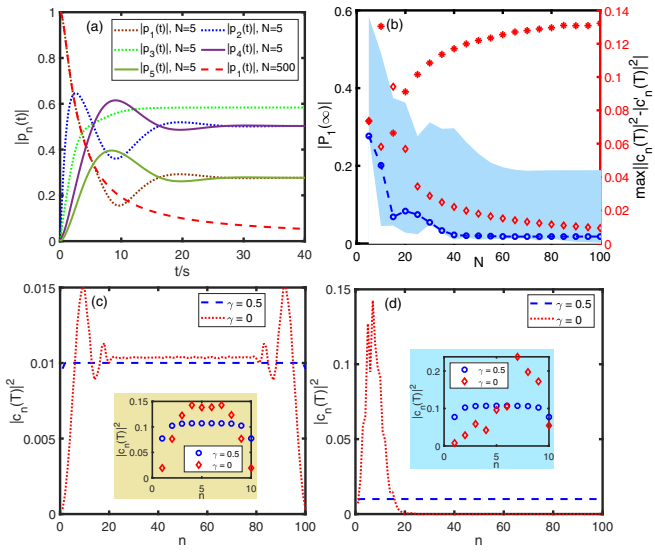

FIG. 4. (a) Comparison of the probability of trapping at different localized sites with two different single-layer trapping methods. $U_0 = 2$ in both of simulations, $v_{nj} = 0.4|x_n - x_j|^{-3}$, $x_n = 0.1n$, $N = 5$ for discrete trapping, and the discrete trapping converges to the continuous case when $N = 500$. (b) The blue-dashed circle evaluated by the left y axis represents the steady value of P_1 between $\max_n(P_n)$ and $\min_n(P_n)$ with the same parameters as (a), and decreases with the increase of lattice sites. The diamond is for the cooperative shielding that $|\psi(0)\rangle = 1/\sqrt{N}\sum_{n=1}^{N}|n\rangle$, the asterisk is for that $|\psi(0)\rangle = 1/\sqrt{5}\sum_{n=1}^{5}|n\rangle$, and both of the two simulations are evaluated by the right y axis. (c) Comparison of cooperative shielding with $|c_n(T)|$ when $|\psi(0)\rangle = 1/\sqrt{N}\sum_{n=1}^{N}|n\rangle$ between $N = 100$ (almost continuous trapping) and $N = 10$ (inset, discrete trapping). (d) Comparison when $|\psi(0)\rangle = 1/\sqrt{5}\sum_{n=1}^{5}|n\rangle$. In (b)–(d), $V = 1$ and $U_0 = 0.1$.

initial state $|\psi(0)\rangle$ and the Hamiltonian [66,67]

$$H_N = -V\sum_n (|n\rangle\langle n+1| + \text{H.c.}) - \sum_{n\neq j}\gamma_{nj}|n\rangle\langle j| - U_0\sum_n |n\rangle\langle n|, \tag{23}$$

where V is the amplitude for nearest-neighbor hopping, γ_{nj} denotes long-range interactions between the nth and jth lattices, and U_0 is the energy of the polar molecules on the site n. The influence by γ_{nj} can be evaluated with the cooperative shielding effect [66–68], which can also be assessed by the occupation $c_n(T)$ at the terminal time point T.

We first consider a simplified case that $\gamma_{nj} \equiv \gamma$, and then consider a general case. As shown in Fig. 4(b), where $c_n(T)$ is for $\gamma \neq 0$ and $c'_n(T)$ is for $\gamma = 0$ [66], the effect of γ can be evaluated with $\max_n ||c_n(T)|^2 - |c'_n(T)|^2|$. The comparisons shown in Figs. 4(c) and 4(d) reveal that the long-range interactions among trapped polar molecules can be canceled out when the number of trapped sites is large based on the designed initial condition.

According to the conclusion in Refs. [66,67], we choose the initial quantum state as a random superposition. For the Hamiltonian given in Eq. (23), the quantum states with N localized sites can be represented as

$$|\psi(t)\rangle = \sum_{n=1}^{N} c_n(t)|n\rangle, \tag{24}$$

where $c_n(t)$, as a generalization of p_n in Eq. (15), represents the amplitude when the nth site is occupied. For the single-layer trapped polar molecules with a single SAW layer and external electric fields, N can be finite. When the polar molecules are trapped with two SAW layers, as in Fig. 3(a), N can be infinitely large.

Given the Hamiltonian as Eq. (23), the evolution of the amplitudes can be written according to the Schrödinger equation $|\dot{\psi}(t)\rangle = -iH_N|\psi(t)\rangle$ as [66]

$$\dot{c}_n(t) = iVc_{n+1}(t) + iVc_{n-1}(t) + i\sum_{n\neq j}\gamma_{nj}c_j(t) + iU_0c_n(t), \tag{25}$$

with $\hbar = 1$. In Fig. 5, we compare the dynamics of Eq. (25) with different number of sites and different initial conditions. The simulations clarify that the long-range interactions can affect the dynamics of the lattices, but it is related to the initial condition and number of sites. If the lattices are initially random or uniformly occupied, the influence of long-range interactions is much smaller or better shielded than the case that a small subset of lattices are initially occupied.

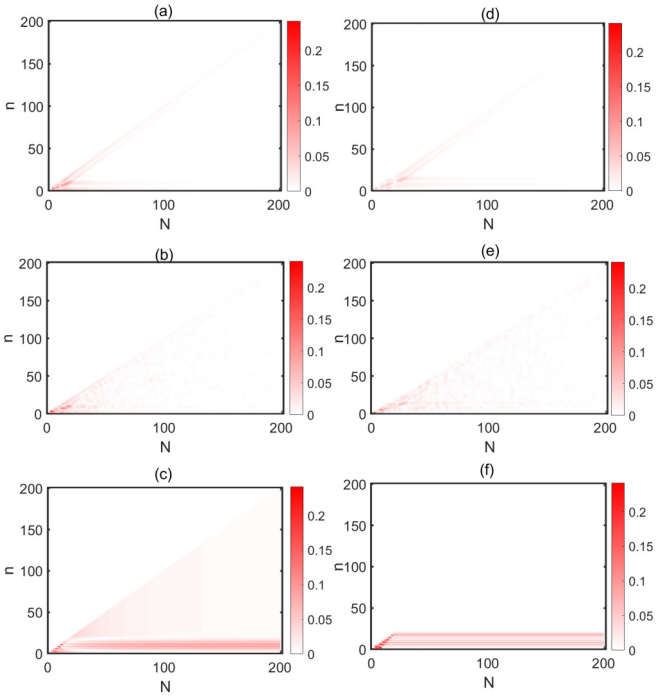

FIG. 5. $||c_n(T)|^2 - |c'_n(T)|^2|$ varies with the number of cites N, where $c_n(T)$ represents the terminal values in Eq. (25) with $\gamma_{nj} = 0$ at $T = 10$ s, and $c'_n(T)$ represents that when $\gamma_{nj} \neq 0$. In all the simulations, $V = 1$ and $U_0 = 0.1$. In (a)–(c), $\gamma_{nj} \equiv \gamma = 2$, and in (d)–(f), $\gamma_{nj} = V|n-j|^{-3}$. In (a) and (d), $c_n(0) = 1/\sqrt{N}$. In (b) and (e), $c_n(t)$ and $c'_n(t)$ are randomly initialized. In (c) and (f), $c_1(0) = c_2(0) = 1/\sqrt{2}$ and $c_n(0) = 0$ for $n > 2$.

V. BOSE-HUBBARD MODEL FOR TRAPPED MOLECULES

When $\bar{u}_2 \gg \bar{u}_1 > 0$, the polar molecules can be trapped in the single-layer lattices by $\bar{u}_2$ and external electric force. This is similar to the purple-dashed curve shown in Fig. 3(b) by replacing z with $D - z$. The energy of the molecules is affected by electric potential of the lower SAW, and the one-dimensional lattice of trapped polar molecules can be described by the Bose-Hubbard model with the Hamiltonian [69–71]

$$H = \int \mathbf{\Psi}^\dagger(\vec{r})\left[-\frac{\hbar^2\nabla^2}{2m_0} + V_e(\vec{r})\right]\mathbf{\Psi}(\vec{r}) + \int \mathbf{\Psi}^\dagger(\vec{r})\mathbf{\Psi}^\dagger(\vec{r'})V(\vec{r}-\vec{r'})\mathbf{\Psi}(\vec{r'})\mathbf{\Psi}(\vec{r})\mathrm{d}^3\vec{r}\mathrm{d}^3\vec{r'}, \quad (26)$$

where m_0 is the mass of the polar molecule, $V_e(\vec{r})$ is the electric potential by the lower SAW, and $\mathbf{\Psi}(\vec{r})$ is a boson field operator for the trapped polar molecules. The field operator $\mathbf{\Psi}(\vec{r})$ can be represented as a superposition of Wannier functions localized at the trapped lattice sites as

$$\mathbf{\Psi}(\vec{r}) = \sum_\mu \hat{a}_\mu w(\vec{r} - \vec{r}_\mu), \quad (27)$$

where the operator $\hat{a}_\mu$ annihilates a polar molecule at the μth site with $\vec{r}_\mu$, and w is the Wannier function, which is determined by the distance between $\vec{r}$ and $\vec{r}_\mu$.

When we only consider the nearest-neighbor interaction between lattices, the trapped polar molecules can be described by the one-dimensional Bose-Hubbard model as [43,72–76]

$$H_B = -J\sum_{\mu,\nu}\hat{a}_\mu^\dagger\hat{a}_\nu + \frac{U}{2}\sum_\mu \hat{n}_\mu(\hat{n}_\mu - 1) + \sum_\mu \epsilon\hat{n}_\mu, \quad (28)$$

where $\hat{a}_\mu(\hat{a}_\mu^\dagger)$ annihilates (creates) a polar molecule at the μth site obeying the canonical commutation relation $[\hat{a}_\nu, \hat{a}_\mu^\dagger] = \delta_{\nu\mu}$, $\hat{n}_\mu = \hat{a}_\mu^\dagger\hat{a}_\mu$, J represents the hopping amplitude between two lattice sites [77], U is the on-site repulsion, and ϵ represents the energy offset of each lattice site affected by $\bar{u}_1$ [43,71,75].

The parameters in Eq. (28) are determined by different lattice sites μ and ν, and can be given as [71]

$$J_{\mu\nu} = \int w^*(\vec{r} - \vec{r}_\mu)\left[-\frac{\hbar^2\nabla^2}{2m_0} + V_e(\vec{r})\right]w(\vec{r} - \vec{r}_\nu)\mathrm{d}^3\vec{r},$$
$$U = \frac{4\pi}{m_0}\int |w(\vec{r})|^4\mathrm{d}^3\vec{r},$$
$$\epsilon_\mu = \int V_e(\vec{r})|w(\vec{r} - \vec{r}_\mu)|^2\mathrm{d}^3\vec{r}, \quad (29)$$

where $V_e(\vec{r})$ is the electric potential induced by the trapping IDT as in Eqs. (A46) and (A48) (see Appendix A). The Wannier function can be approximately simplified with the Gaussian function as $w(x) = e^{-x^2/2}$ [78–80]. When $|\mu - \nu| = 1$ in Eq. (29), $J_{\mu\nu}$ reduces to J for the simplified nearest-neighbor case in Eq. (28).

Above all, the lattice network is determined by the spatial distribution of the external force, and the number of lattice sites can be arbitrarily manipulated. If we only consider a short timescale that $k(x - vt)$ varies a little, as the practical case in Refs. [20,36,52,56], or the theoretical estimation in Ref. [43] that the tunneling time among lattices and the time for the occurrence of lattice dynamics vary from 10 ps to 15 ns, then Eq. (29) can be simplified to

$$\begin{aligned} J_{\mu\nu} &= \int e^{-(x-x_\mu)^2/2}\left\{-\frac{\hbar^2\nabla^2}{2m_0} + B_0e^{-kz}\cos[k(x - vt)]\right\}e^{-(x-x_\nu)^2/2}\mathrm{d}x \\ &\approx \Delta\left(\frac{1-\Delta^2}{2m_0} + B_0e^{-kz}\cos[k(x - vt)]\right)e^{-\Delta^2} \\ &\approx \Delta\left(\tilde{B}_0e^{-kz} + \delta_J\right)e^{-\Delta^2} \\ &\triangleq J, \end{aligned} \quad (30)$$

where Δ is the distance between two nearest-neighbor lattice sites, $\hbar = 1$ for simplification, then we regard the time-domain evolution as a bounded perturbation as δ_J [77]. Similarly,

$$\begin{aligned} U &= \frac{4\pi}{m_0}\int e^{-2x^2}\mathrm{d}x, \\ \epsilon &= B_0e^{-kz}\cos[k(x_\nu - vt)] \approx (\tilde{B}_0 + \delta_\epsilon)e^{-kz}, \end{aligned} \quad (31)$$

where δ_ϵ is a bounded perturbation similarly as in Eq. (30) within a short timescale. In the following, we first study a simplified case with $\delta_J = \delta_\epsilon = 0$ and then generalize to the case that $\delta_J, \delta_\epsilon \neq 0$.

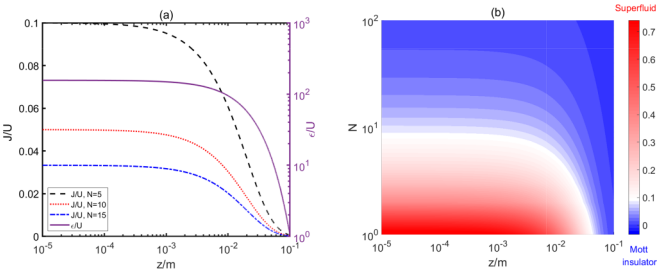

FIG. 6. (a) J/U and ϵ/U affected by the trapped height z of polar molecules. The distance between two nearest-neighbor sites is $\Delta = 0.005/N$m with $N = 5, 10, 15$ representing the number of lattice sites, $\delta_J = \delta_\epsilon = 0$, $m_0 = 0.1$, $\tilde{B}_0 = 100$ and $k = 50$. (b) The phase transition evaluated by J/U between the Mott insulator and superfluid affected by the trapped height and the number of lattice sites. In the simulation, $k = 50$, the polar molecules are trapped by the IDT array with a horizontal width of 0.005 m, $n_0 = 1$ and $f_{n_0} = 0.085786$.

In Fig. 6, J/U and ϵ/U are plotted as functions of z, which is the distance between the trapped polar molecules and the lower SAW. It can be seen that both J/U and ϵ/U decrease with the increase in z. This is because of the fact that the electric potential by the lower SAW decreases with the increase in z. Using this, we can modulate the transition between different phases of the Bose-Hubbard model as follows.

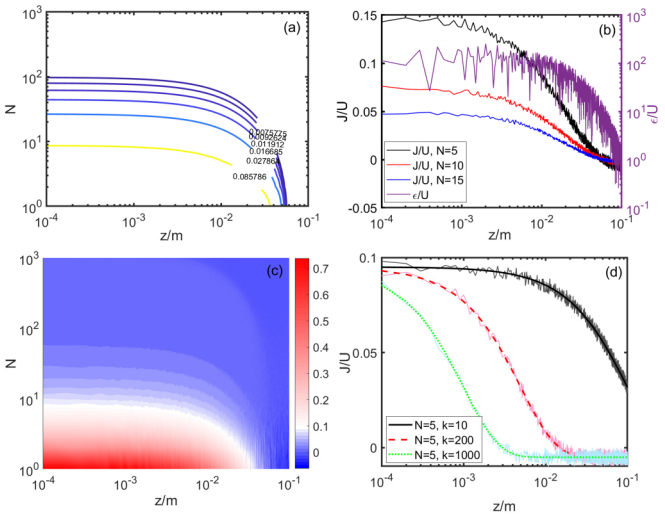

FIG. 7. (a) Phase transition boundaries when $n_0 = 1, 4, 7, 10, 13, 16$ and $f_{n_0} = 0.085786, 0.027864, \cdots, 0.0075775$, respectively. (b) The parameters of the Bose-Hubbard model affected by random components $\delta_J \in [-5, 5]$ and $\delta_\epsilon \in [-100, 100]$. (c) The phase transition between superfluid (red) and Mott insulator (blue) evaluated by J/U with the uncertain parameters in (b). (d) J/U affected by the wave number k when $N = 5$ and $\delta_J \in [-5, 5]$. In all the simulations, $\tilde{B}_0 = 100$, the distance between two nearest-neighbor trapped polar molecules is $0.005/N$m, and $k = 50$ in (a)–(c).

The transition between the superfluid and Mott insulator is determined by J/U and the average number of molecules n_0 at each lattice site [81]. According to the conclusion in Refs. [81,82], the transition boundary between the superfluid and Mott insulator occurs when $\epsilon/U - n_0 = -1/2 - J/U \pm \sqrt{(J/U)^2 - (2n_0+1)J/U + 1/4}$, then the polar molecule gas will be superfluid when $J/U > n_0 + 1/2 - \sqrt{n_0(n_0+1)} \triangleq f_{n_0}$, where $n_0 = 1, 2, \cdots$ represent the mean polar molecule number in the trapped lattice sites. For example, when $n_0 = 1$, $f_{n_0} = 0.085786$, corresponds to the case in Fig. 6(b). The relationship between the designed J/U and ϵ can affect the transition between the superfluid ($J/U > f_{n_0}$) and Mott insulator ($J/U < f_{n_0}$) [75,83–85]. Thus by controlling the trapped position of polar molecules along z direction and the number of lattice sites, the transition between the superfluid and Mott insulator can be manipulated as in Fig. 6(b). In this transition, the exponential decay of the electric potential induced by SAW in the open space along the z-direction plays a crucial role, and makes it possible for the transition occurrence with varied numbers of lattice sites, which is the special property provided by the acoustic wave when compared with traditional modulating methods [21–24].

Additionally, the transition process is also affected by n_0 and the uncertainties induced by time dependent potential if we only consider a quite short time period. In such cases, the molecules are trapped in the lattices as in experimental circumstance in Ref. [20], and are also affected by the thermal effect determined by the environment temperature. The phase transition needs to be further analyzed as follows.

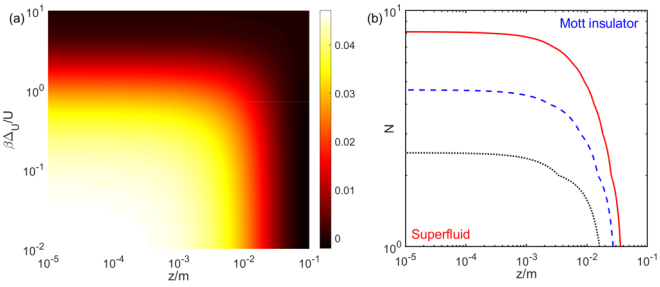

FIG. 8. (a) J_T/U affected by the temperature when $N = 10$ and other parameters are same as Fig. 6(a). (b) The phase transition boundary between superfluid and Mott insulator for $n_0 = 1$ affected by different temperatures with $\beta\Delta_U = 0.1U$(solid-red), U(dashed-blue), and $2U$(dotted-black), respectively.

A. Influence of n_0, uncertainties, and thermal effects

For a general case of n_0, the contours in Fig. 7(a) represent the phase transition boundary when $n_0 = 1, 4, 7, 10, 13, 16$, where f_{n_0} decreases with the increase of n_0. Thus when n_0 is larger, it is easier to generate the superfluid state. Figure 7(b) shows the parameters with random oscillations, and Fig. 7(c) shows the phase transition affected by the parameters in Fig. 7(b) when $n_0 = 1$. It can be seen that the parameter oscillations can induce some errors but not destruct the overall transition property mainly affected by the trapped height of the polar molecule array and the number of lattice sites.

Besides, the thermal effects can affect the hopping of polar molecules among different lattice sites, and this will further affect the parameter J in the Bose-Hubbard model in Eq. (28) as $J_T = Je^{-\beta\Delta_U}$ [86–88], where β is the temperature, Δ_U is a constant, and $\beta\Delta_U$ can be evaluated according to U in the Bose-Hubbard model. Then the evolutions of lattices are governed by Eq. (28) after replacing J with J_T. As illustrated in Fig. 8(a), the thermal effect can affect the parameter J_T/U, together with the trapped height, and this can further affect the phase transitions of the trapped polar molecule gas. As compared in Fig. 8(b), the lower temperature is easier for the construction of superfluid state, and stronger thermal effect can induce Mott insulator.

B. Influence of the wave number

For different wave numbers of the acoustic wave, the phase transition boundaries are different. As shown in Eq. (A51) and Fig. 7(d), the amplitudes of the electric field and the electric force by SAW decrease along the z direction at the rate determined by the wave number k. When k is small, the transition between the Mott insulator and superfluid is mainly determined by the number of lattice sites, as shown in Figs. 9(a) and 9(d). In this case, when N is small, the molecule array can mainly be the superfluid if the molecules are only trapped close to the electrodes on the piezoelectric material with surface acoustic waves. However, when k is large, the electric potential decreases fast with the increase of z. Thus when N is small, the transition between the superfluid and Mott insulator can also occur when k is large enough, as shown in Figs. 9(b)–9(f).

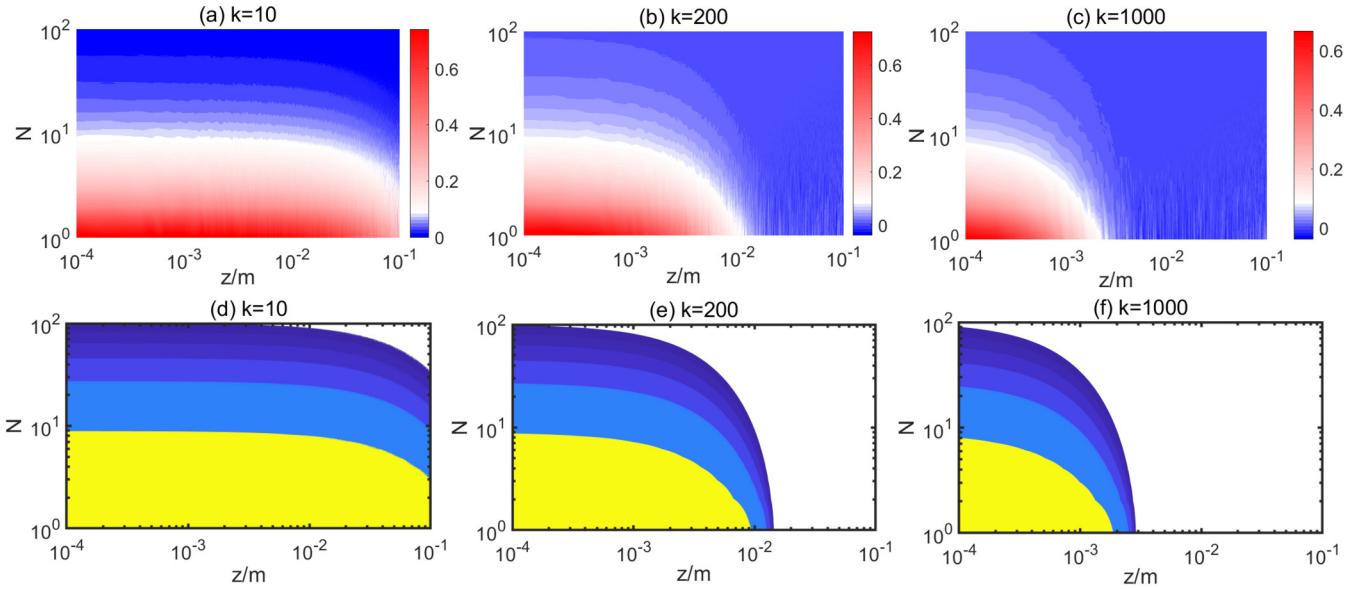

FIG. 9. The influence on the phase transition by the wave number k of the acoustic wave. (a)–(c) represent the phase transition between the superfluid (red region) and Mott insulator (blue region) with $n_0 = 1$ and the uncertainties in Fig. 7(b). (d)–(f) represent the phase transition boundaries with $n_0 = 1, 4, 7, 10, 13, 16$, and different colors represent the regions for the superfluid state separated by the boundaries with different n_0 compared with the white insulator region. In all the simulations, $B_0 = 100$, the distance between two nearest neighbor trapped polar molecules is $0.005/N$m.

VI. CONCLUSIONS

We have proposed a method to trap polar molecules with the electric field induced by surface acoustic waves. Assisted by external electric fields, the polar molecules can be trapped and arranged into single or multiparallel layers away from the piezoelectric material. Depending on the uniformity of the layers in the longitudinal direction, the attractive interactions among the molecules in each layer can be different, which can further affect the binding energy of the trapped polar molecule array. For a single layer of trapped polar molecules, the final steady distribution of the molecules can be affected by the trapping approach with finite or infinite lattice sites. The trapped polar molecules can be used to construct the lattice based Bose-Hubbard model. The phase transition between the superfluid and Mott insulator can be controlled by designing the values and spatial distributions of the external electric force. The advantages of SAW for trapping polar molecules are that its induced electric field satisfies the condition of stability for trapping a polar particle, the field can be real-time modulated by the electric field applied to the input IDT, and arbitrary three-dimensional polar molecule lattices can in principle be trapped by tuning another applied electric force. Our proposal can be more efficient compared with traditional trapping methods with electric force such as in Refs. [21–24]. Besides, the exponential decrease of the electric field produced by SAW along the vertical direction in the open space can induce the transition between Mott insulator and superfluid, and the overall architecture can be fabricated on-chip with extensive possible expansions. From the perspective of experimental realization, the deceleration of the molecule gas has been realized in Refs. [20,52,89], the on-chip design of the surface acoustic wave resonator has been demonstrated in Ref. [53], and the method of shaping electric fields in the open space between two SAW layers has been introduced in Refs. [21,54]. These technologies support the viability of the proposed trapping method. Our proposal has potential applications in the construction of superfluid and Mott insulator [90,91], phase transitions [92–94], lattice QED [74,95], as well as quantum information processing [96]. This might open an easy way to hybridize molecules with solid-state quantum devices, in contrast to trapping molecules using optical lattices.

ACKNOWLEDGMENT

Y.X.L. is supported by the National Science Foundation of China (NSFC) under Grants No. 12374483 and No. 92365209. R.B.W. is supported by the NSFC under Grants No. 61833010 and No. 62173201.

APPENDIX A: CALCULATIONS ON THE SURFACE ACOUSTIC WAVE

Assume the displacement of the piezoelectric material is $\mathbf{u} = (u_1, u_2, u_3)$ at the position $\vec{r} = [x_1, x_2, x_3]^T$. When there are not any strains in the material, the material moves as a whole and the displacement at $\vec{r}$ and $\vec{r'}$ satisfies that

$$\mathbf{u}(\vec{r}) = \mathbf{u}(\vec{r'}), \tag{A1}$$

and

$$\frac{\partial u_i}{\partial x_j} = 0, \quad \forall i, j = 1, 2, 3. \tag{A2}$$

The strain at $\vec{r}$ is defined as

$$S_{ij}(x_1, x_2, x_3) = \frac{1}{2}\left(\frac{\partial u_i}{\partial x_j} + \frac{\partial u_j}{\partial x_i}\right),\ i, j = 1, 2, 3. \tag{A3}$$

If the material is not piezoelectric, the motion of a single unit satisfies that [40]

$$\rho\frac{\partial^2 u_i}{\partial t^2} = \sum_j \frac{\partial T_{ij}}{\partial x_j},\ i, j = 1, 2, 3, \tag{A4}$$

where ρ is the density, T is the stress. Here T is proportional to the strain S if the inner force is small, namely

$$T_{ij} = \sum_k \sum_l c_{ijkl} S_{kl},\ i, j, k, l = 1, 2, 3, \tag{A5}$$

where $S_{kl} = \partial u_k/\partial x_l$, the parameters c_{ijkl} are regarded as the stiffness tensor and can be replaced with the matrix $\mathbf{C}$ as

$$\mathbf{C} = \begin{bmatrix} c_{11} & c_{12} & c_{12} & 0 & 0 & 0 \\ c_{12} & c_{11} & c_{12} & 0 & 0 & 0 \\ c_{12} & c_{12} & c_{11} & 0 & 0 & 0 \\ 0 & 0 & 0 & c_{44} & 0 & 0 \\ 0 & 0 & 0 & 0 & c_{44} & 0 \\ 0 & 0 & 0 & 0 & 0 & c_{44} \end{bmatrix}$$

with the corresponding relationship between c_{ijkl} and $\mathbf{C}$ introduced in Ref. [40].

1. Solutions for isotropic materials

In the isotropic material

$$c_{ijkl} = \kappa\delta_{ij}\delta_{kl} + \mu(\delta_{ik}\delta_{jl} + \delta_{il}\delta_{jk}), \tag{A6}$$

where κ and μ are positive Lam*é* constants and the Kronecker delta function is defined as $\delta_{ij} = 1$ when $i = j$ and $\delta_{ij} = 0$ when $i \neq j$. The stress T can be calculated as

$$\begin{aligned} T_{ij} &= \sum_k \sum_l c_{ijkl} S_{kl} \\ &= \sum_k \sum_l (\kappa\delta_{ij}\delta_{kl} + \mu(\delta_{ik}\delta_{jl} + \delta_{il}\delta_{jk}))S_{kl} \\ &= \sum_k \sum_l \kappa\delta_{ij}\delta_{kl}S_{kl} + \sum_k \sum_l \mu(\delta_{ik}\delta_{jl} + \delta_{il}\delta_{jk})S_{kl} \\ &= \sum_k \kappa\delta_{ij}S_{kk} + \sum_k \sum_l \mu(\delta_{ik}\delta_{jl} + \delta_{il}\delta_{jk})S_{kl} \\ &= \sum_k \kappa\delta_{ij}S_{kk} + 2\mu S_{ij}, \end{aligned} \tag{A7}$$

where

$$S_{kk} = \frac{\partial u_k}{\partial x_k}. \tag{A8}$$

Denote $\Delta = \sum_k S_{kk}$, then

$$T_{ij} = \kappa\delta_{ij}\Delta + 2\mu S_{ij}. \tag{A9}$$

Equation (A4) can then be written as

$$\begin{aligned} \rho\frac{\partial^2 u_i}{\partial t^2} &= \sum_j \frac{\partial T_{ij}}{\partial x_j} \\ &= \frac{\partial \kappa\Delta}{\partial x_i} + 2\mu\sum_j \frac{\partial S_{ij}}{\partial x_j} \\ &= \kappa\frac{\partial \Delta}{\partial x_i} + 2\mu\sum_j \frac{\frac{1}{2}\left(\frac{\partial u_i}{\partial x_j} + \frac{\partial u_j}{\partial x_i}\right)}{\partial x_j} \\ &= \kappa\frac{\partial \Delta}{\partial x_i} + \mu\sum_j \frac{\partial^2 u_j}{\partial x_i \partial x_j} + \mu\sum_j \frac{\partial^2 u_i}{\partial x_j^2} \\ &= \kappa\frac{\partial \Delta}{\partial x_i} + \mu\frac{\partial\left(\sum_j \partial u_j/\partial x_j\right)}{\partial x_i} + \mu\nabla^2 u_i \\ &= (\kappa + \mu)\frac{\partial \Delta}{\partial x_i} + \mu\nabla^2 u_i, \end{aligned} \tag{A10}$$

where $\nabla^2 = \sum_i \frac{\partial^2}{\partial x_i^2}$ and $i, j = 1, 2, 3$.

The components of Eq. (A10) read

$$\begin{aligned} \rho\frac{\partial^2 u_1}{\partial t^2} &= (\kappa + \mu)\frac{\partial(S_{11} + S_{22} + S_{33})}{\partial x_1} + \mu\nabla^2 u_1 \\ &= (\kappa + 2\mu)\frac{\partial^2 u_1}{\partial^2 x_1} + (\kappa + \mu)\left(\frac{\partial^2 u_2}{\partial x_2 \partial x_1} + \frac{\partial^2 u_3}{\partial x_3 \partial x_1}\right) \\ &\quad + \mu\left(\frac{\partial^2 u_1}{\partial^2 x_2} + \frac{\partial^2 u_1}{\partial^2 x_3}\right), \end{aligned} \tag{A11}$$

$$\begin{aligned} \rho\frac{\partial^2 u_2}{\partial t^2} &= (\kappa + 2\mu)\frac{\partial^2 u_2}{\partial^2 x_2} + (\kappa + \mu)\left(\frac{\partial^2 u_1}{\partial x_2 \partial x_1} + \frac{\partial^2 u_3}{\partial x_3 \partial x_2}\right) \\ &\quad + \mu\left(\frac{\partial^2 u_2}{\partial^2 x_1} + \frac{\partial^2 u_2}{\partial^2 x_3}\right), \end{aligned} \tag{A12}$$

and

$$\begin{aligned} \rho\frac{\partial^2 u_3}{\partial t^2} &= (\kappa + 2\mu)\frac{\partial^2 u_3}{\partial^2 x_3} + (\kappa + \mu)\left(\frac{\partial^2 u_1}{\partial x_3 \partial x_1} + \frac{\partial^2 u_2}{\partial x_3 \partial x_2}\right) \\ &\quad + \mu\left(\frac{\partial^2 u_3}{\partial^2 x_1} + \frac{\partial^2 u_3}{\partial^2 x_2}\right). \end{aligned} \tag{A13}$$

The vector format of the displacement $\mathbf{u} = [u_1, u_2, u_3]^T$ can be represented as [97]

$$[u_1, u_2, u_3]^T = [\bar{U}, \bar{V}, \bar{W}]^T e^{-kqx_3 + ik(lx_1 + mx_2 - vt)}, \tag{A14}$$

where $\bar{U}$, $\bar{V}$, and $\bar{W}$ are constants determined by q representing the possible decay in the direction of x_3, k is the wave number, v is the velocity of the acoustic wave, $l = \cos\theta$, $m = \sin\theta$, θ is the angle between the propagating direction of the wave front with the x_3 axis. Thus l and m can represent the propagating direction of the acoustic wave. Taking Eq. (A14) into Eqs. (A11)–(A13), we have $\mathbf{P}(q)[\bar{U}\ \bar{V}\ i\bar{W}]^T = 0$ with the matrix [98]

$$\mathbf{P}(q) = \begin{bmatrix} P_{11} & (\kappa + \mu)lm & (\kappa + \mu)lq \\ (\kappa + \mu)lm & P_{22} & (\kappa + \mu)mq \\ (\kappa + \mu)lq & (\kappa + \mu)mq & P_{33} \end{bmatrix}, \tag{A15}$$

where $P_{11} = (\kappa + 2\mu)l^2 - v^2\rho + \mu(m^2 - q^2)$, $P_{22} = (\kappa + 2\mu)m^2 - v^2\rho + \mu(l^2 - q^2)$, $P_{33} = (\kappa + 2\mu)q^2 +$

$v^2\rho - \mu(l^2+m^2)$, $l^2+m^2=1$. Take $\det(\mathbf{P}(q))=0$, and we can denote the solutions of q as q_1, q_2, q_3.

2. Solutions for piezoelectric materials

If the material is piezoelectric, the stress is also determined by the external electric field, namely [40]

$$T_{ij} = \sum_k \sum_l c_{ijkl} S_{kl} - \sum_k e_{kij} E_k,\ i,j,k,l = 1,2,3, \tag{A16}$$

where the electric field E_k is applied along the x axis. Assume the electric potential is Φ, the electric field satisfies that $E_k = -\partial\Phi/\partial x_k$. Thus the motion equation within the piezoelectric materials reads

$$\begin{aligned}
\rho\frac{\partial^2 u_i}{\partial t^2} &= \sum_j \frac{\partial T_{ij}}{\partial x_j} \\
&= \sum_j \frac{\partial\left(\sum_k\sum_l c_{ijkl}S_{kl} - \sum_k e_{kij}E_k\right)}{\partial x_j} \\
&= \sum_j\sum_k e_{kij}\frac{\partial^2\Phi}{\partial x_j\partial x_k} + \sum_j\sum_k\sum_l c_{ijkl}\frac{\partial S_{kl}}{\partial x_j} \\
&= \sum_j\sum_k e_{kij}\frac{\partial^2\Phi}{\partial x_j\partial x_k} + \frac{1}{2}\sum_j\sum_k\sum_l c_{ijkl}\frac{\partial\left(\frac{\partial u_k}{\partial x_l} + \frac{\partial u_l}{\partial x_k}\right)}{\partial x_j} \\
&= \sum_j\sum_k e_{kij}\frac{\partial^2\Phi}{\partial x_j\partial x_k} \\
&\quad + \frac{1}{2}\sum_j\sum_k\sum_l c_{ijkl}\left(\frac{\partial^2 u_k}{\partial x_l\partial x_j} + \frac{\partial^2 u_l}{\partial x_k\partial x_j}\right) \\
&= \sum_j\sum_k e_{kij}\frac{\partial^2\Phi}{\partial x_j\partial x_k} + \frac{1}{2}\sum_j\sum_k\sum_l c_{ijkl}\frac{\partial^2 u_k}{\partial x_l\partial x_j} \\
&\quad + \frac{1}{2}\sum_j\sum_k\sum_l c_{ijkl}\frac{\partial^2 u_l}{\partial x_k\partial x_j}.
\end{aligned} \tag{A17}$$

Because $S_{kl} = S_{lk}$ and $T_{ij} = T_{ji}$, then

$$\frac{\partial^2 u_k}{\partial x_l\partial x_j} = \frac{\partial^2 u_l}{\partial x_k\partial x_j}, \tag{A18}$$

and

$$\rho\frac{\partial^2 u_i}{\partial t^2} = \sum_j\sum_k e_{kij}\frac{\partial^2\Phi}{\partial x_j\partial x_k} + \sum_j\sum_k\sum_l c_{ijkl}\frac{\partial^2 u_k}{\partial x_l\partial x_j}. \tag{A19}$$

The piezoelectric material is considered to be an insulator with $\int_v \nabla\cdot\mathbf{D}dv = 0$, and $\mathbf{D} = [D_i, D_j, D_k]$ with $D_i = D_j = 0$, then

$$\begin{aligned}
div\mathbf{D} &= \frac{\partial D_i}{\partial x_i} + \frac{\partial D_j}{\partial x_j} + \frac{\partial D_k}{\partial x_k} \\
&= -\sum_j \varepsilon^S_{kj}\frac{\partial^2\Phi}{\partial x_j\partial x_k} + \frac{1}{2}\sum_i\sum_j e_{ijk}\left(\frac{\partial^2 u_i}{\partial x_j\partial x_k} + \frac{\partial^2 u_j}{\partial x_i\partial x_k}\right),
\end{aligned} \tag{A20}$$

where

$$\begin{aligned}
D_k &= \sum_j \varepsilon^S_{kj}E_j + \sum_i\sum_j e_{ijk}S_{ij} \\
&= -\sum_j \varepsilon^S_{kj}\frac{\partial\Phi}{\partial x_j} + \frac{1}{2}\sum_i\sum_j e_{ijk}\left(\frac{\partial u_i}{\partial x_j} + \frac{\partial u_j}{\partial x_i}\right).
\end{aligned} \tag{A21}$$

Because i and j are in the symmetric positions as $\partial^2 u_i/\partial x_j/\partial x_k = \partial^2 u_j/\partial x_i/\partial x_k$, then

$$div\mathbf{D} = -\sum_j \varepsilon^S_{kj}\frac{\partial^2\Phi}{\partial x_j\partial x_k} + \sum_i\sum_j e_{ijk}\frac{\partial^2 u_i}{\partial x_j\partial x_k}. \tag{A22}$$

Then

$$\sum_k\left(\sum_i\sum_j e_{ijk}\frac{\partial^2 u_i}{\partial x_j\partial x_k} - \sum_j \varepsilon^S_{kj}\frac{\partial^2\Phi}{\partial x_j\partial x_k}\right) = 0. \tag{A23}$$

Because of the piezoelectric property, the boundary condition reads

$$\begin{aligned}
T_{iz} &= \sum_k\sum_l c_{izkl}S_{kl} - \sum_k e_{kiz}E_k \\
&= \sum_k\sum_l c_{izkl}S_{kl} + \sum_k e_{kiz}\frac{\partial\Phi}{\partial x_k} \\
&= \sum_k\sum_l c_{izkl}\frac{1}{2}\left(\frac{\partial u_k}{\partial x_l} + \frac{\partial u_l}{\partial x_k}\right) + \sum_k e_{kiz}\frac{\partial\Phi}{\partial x_k} = 0,
\end{aligned} \tag{A24}$$

where $i,k,l = 1,2,3$ and $z = 0$.

Because $S_{kl} = S_{lk}$, then

$$T_{iz} = \sum_k\sum_l c_{izkl}\frac{\partial u_k}{\partial x_l} + \sum_k e_{kiz}\frac{\partial\Phi}{\partial x_k} = 0, \tag{A25}$$

which means that there are no mechanical forces in arbitrary directions on the free surface, namely $T_{zx} = T_{zy} = T_{zz} = 0$ at $z = 0$. Then Eq. (A25) can be rewritten as

$$c_{izkl}\frac{\partial u_k}{\partial x_l} + e_{kiz}\frac{\partial\Phi}{\partial x_k} = 0,\ \forall i,k,l = 1,2,3. \tag{A26}$$

Above all, the equations of the acoustic field can be written as

$$\begin{aligned}
&\rho\frac{\partial^2 u_i}{\partial t^2} = \sum_j\sum_k e_{kij}\frac{\partial^2\Phi}{\partial x_j\partial x_k} + \sum_j\sum_k\sum_l c_{ijkl}\frac{\partial^2 u_k}{\partial x_l\partial x_j}, \\
&\sum_k\left(\sum_i\sum_j e_{ijk}\frac{\partial^2 u_i}{\partial x_j\partial x_k} - \sum_j \varepsilon^S_{kj}\frac{\partial^2\Phi}{\partial x_j\partial x_k}\right) = 0, \\
&c_{izkl}\frac{\partial u_k}{\partial x_l} + e_{kiz}\frac{\partial\Phi}{\partial x_k} = 0,
\end{aligned} \tag{A27}$$

where the second line is the electric boundary condition with $z = 0$, and the third line is the mechanical boundary condition with $z = 0$, which means that the stress is free at the boundary. Then in Eq. (A4), $T_{i3} = 0$ when $z = 0$ for $i = 1,2,3$.

Based on the model above, we have the time-dependent strain field S_{kl} and the electric potential Φ satisfying that

$$\frac{\partial^2\Phi}{\partial x_j\partial x_k} = -\frac{c_{izkl}}{e_{kiz}}\frac{\partial^2 u_k}{\partial x_l\partial x_j}. \tag{A28}$$

The motion of the piezoelectric material reads

$$\rho\frac{\partial^2 u_i}{\partial t^2} = -\sum_j\sum_k e_{kij}\frac{c_{izkl}}{e_{kiz}}\frac{\partial^2 u_k}{\partial x_l \partial x_j} + \sum_j\sum_k\sum_l c_{ijkl}\frac{\partial^2 u_k}{\partial x_l \partial x_j}. \tag{A29}$$

Besides, Eq. (A16) can also be written as

$$S_{ij} = \sum_k\sum_l s_{ijkl}T_{kl} + \sum_k d_{kij}E_k,\ i,j,k,l = 1,2,3, \tag{A30}$$

where d_{kij} is given according to e_{14} in Eq. (A29) and can be represented with the matrix $\mathbf{d}$ with $k = 1, 2, 3$ for different lines of the matrix as

$$\mathbf{d} = \begin{bmatrix} 0 & 0 & 0 & d_{14} & 0 & 0 \\ 0 & 0 & 0 & 0 & d_{14} & 0 \\ 0 & 0 & 0 & 0 & 0 & d_{14} \end{bmatrix}.$$

In the piezoelectric material, there are only three independent elastic constants for the c_{ijkl} in Eq. (A27) denoted as c_{11}, c_{12}, c_{44} [45]. Then the equation in Eq. (A27) can be simplified and rewritten as

$$\rho\frac{\partial^2 u_x}{\partial t^2} = c_{11}\frac{\partial^2 u_x}{\partial x^2} + c_{44}\left(\frac{\partial^2 u_x}{\partial y^2} + \frac{\partial^2 u_x}{\partial z^2}\right) + (c_{12}+c_{44})\left(\frac{\partial^2 u_y}{\partial x \partial y} + \frac{\partial^2 u_z}{\partial x \partial z}\right) + 2e_{14}\frac{\partial^2 \phi}{\partial y \partial z}, \tag{A31}$$

$$\rho\frac{\partial^2 u_y}{\partial t^2} = c_{11}\frac{\partial^2 u_y}{\partial y^2} + c_{44}\left(\frac{\partial^2 u_y}{\partial x^2} + \frac{\partial^2 u_y}{\partial z^2}\right) + (c_{12}+c_{44})\left(\frac{\partial^2 u_x}{\partial y \partial x} + \frac{\partial^2 u_z}{\partial y \partial z}\right) + 2e_{14}\frac{\partial^2 \phi}{\partial x \partial z}, \tag{A32}$$

$$\rho\frac{\partial^2 u_z}{\partial t^2} = c_{11}\frac{\partial^2 u_z}{\partial z^2} + c_{44}\left(\frac{\partial^2 u_z}{\partial x^2} + \frac{\partial^2 u_z}{\partial y^2}\right) + (c_{12}+c_{44})\left(\frac{\partial^2 u_x}{\partial z \partial x} + \frac{\partial^2 u_y}{\partial z \partial y}\right) + 2e_{14}\frac{\partial^2 \phi}{\partial x \partial y}, \tag{A33}$$

$$\varepsilon\Delta\phi = 2e_{14}\left(\frac{\partial^2 u_x}{\partial y \partial z} + \frac{\partial^2 u_y}{\partial x \partial z} + \frac{\partial^2 u_z}{\partial x \partial y}\right), \tag{A34}$$

where u_x, u_y, and u_z represent the displacements in the three-dimensional coordinate system with the mechanical boundary condition at $z = 0$ reads

$$T_{13} = c_{44}\left(\frac{\partial u_z}{\partial x} + \frac{\partial u_x}{\partial z}\right) + e_{14}\frac{\partial \phi}{\partial y} = 0,$$
$$T_{23} = c_{44}\left(\frac{\partial u_z}{\partial y} + \frac{\partial u_y}{\partial z}\right) + e_{14}\frac{\partial \phi}{\partial x} = 0, \tag{A35}$$
$$T_{33} = c_{11}\frac{\partial u_z}{\partial z} + c_{12}\left(\frac{\partial u_x}{\partial x} + \frac{\partial u_y}{\partial y}\right) = 0,$$

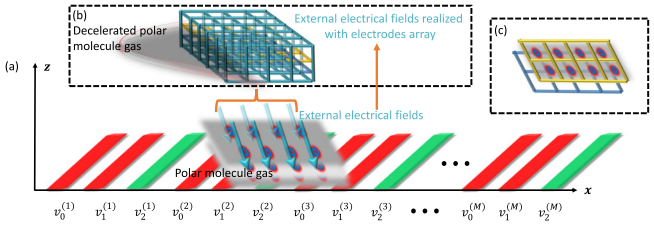

FIG. 10. (a) Schematic diagram for the voltage distributions of the receiving IDT. The polar molecules interact simultaneously with both the electric field from receiving IDT and externally applied control electric field. (b) The physical realization of designed external electric fields in (a) with an array of electrodes. (c) An example of polar molecules trapped in the lattices constructed by the electrodes.

and the electric boundary condition at $z = 0$ reads

$$e_{14}\left(\frac{\partial u_x}{\partial y} + \frac{\partial u_y}{\partial x}\right) - \varepsilon\frac{\partial \phi}{\partial z} + \varepsilon_0 k\phi = 0. \tag{A36}$$

When the sample is fabricated on the polished (100) surface, the acoustic wave propagates along the [011] direction, and is of the format [45,51,98]

$$u_x = \frac{u}{\sqrt{2}}e^{-kz+ik(x+y)/\sqrt{2}-ivkt},$$
$$u_y = \frac{u}{\sqrt{2}}e^{-kz+ik(x+y)/\sqrt{2}-ivkt}, \tag{A37}$$
$$u_z = \tilde{u}_z e^{-kz+ik(x+y)/\sqrt{2}-ivkt}.$$

Equation (A34) reads

$$\varepsilon\Delta\phi = \begin{cases} 2e_{14}\left(2\frac{\partial^2 u_x}{\partial x \partial z} + \frac{\partial^2 u_z}{\partial x^2}\right), & 0 < z < H, \\ 0, & \text{else}, \end{cases} \tag{A38}$$

where H represents the thickness of the IDT fingers, and $\Delta\phi = \partial^2\phi/\partial x^2 + \partial^2\phi/\partial y^2 + \partial^2\phi/\partial z^2$.

Then the electric potential can be represented as

$$\phi = \chi(z)e^{ik(x+y)/\sqrt{2}-ivkt}, \tag{A39}$$

where $\chi(z)$ reads

$$\chi(z) = \begin{cases} \chi_p(z) + B_1 e^{kz} + B_2 e^{-kz}, & 0 < z < H, \\ B_3 e^{kz}, & z \leqslant 0, \\ B_4 e^{-kz}, & z \geqslant H, \end{cases} \tag{A40}$$

which is given in Ref. [51] with the detailed format of $\chi_p(z)$ and B_j with $j = 1, 2, 3, 4$ are to be determined parameters.

The amplitude of the electric field by SAW can be calculated as [99]

$$|\vec{E}(x,y,z)| = \sqrt{\left(\frac{\partial\phi}{\partial x}\right)^2 + \left(\frac{\partial\phi}{\partial y}\right)^2 + \left(\frac{\partial\phi}{\partial z}\right)^2}. \tag{A41}$$

3. Electrical fields induced by the surface acoustic wave

In this section, we introduce the realization of the electric fields interacting with the polar molecules in our proposal. As schematically shown in Fig. 10(a), the polar molecules can simultaneously interact with the electric field by SAW and designed external electric fields. Experimentally, the external electric field can be realized with the three-dimensional

electrode array as in Fig. 10(b) or Ref. [54]. Thus the polar molecules can be trapped in the lattices constructed and controlled by the electric fields of the electrodes such as in Fig. 10(c). Based on the format of the electric potential given in Eqs. (A39) and (A40), the polar molecule can be driven by the electric field with the potential as

$$\phi = \Re\left[B_4 e^{-kz} e^{ik(x+y)/\sqrt{2}-ivkt}\right], \tag{A42}$$

which satisfies that $\Delta\phi = \partial^2\phi/\partial^2 x^2 + \partial^2\phi/\partial^2 y^2 + \partial^2\phi/\partial^2 z^2 = 0$ and $\Re$ represents the real part of a complex value. The surface acoustic wave and polar molecules are coupled via the nonreflective IDT, as shown in Fig. 1. We replace $x+y$ with x in Fig. 10 and the following and the analysis in the main text for simplification, then [98,100,101]

$$\phi(x,z,t) = \Re\left[B_4 e^{-kz} e^{ik(x-vt)}\right] = X(x,t)Z(z), \tag{A43}$$

where

$$X(x,t) = \Re\left[e^{ik(x-vt)}\right], \quad Z(z) = B_4 e^{-kz}. \tag{A44}$$

The period of the receiving IDT is $l = 6p' = \lambda$ where p' is the width of an electrode of the red and green fingers in Fig. 10. Assume the number of periods is M as in Fig. 10 and λ is the wave length of the acoustic wave. For the jth finger in a period with $j = 0, 1, 2$, when the voltage is 1 V on the electrode, the induced potential is

$$\phi_j(x,z,t) = \sum_{m=1}^{M} \phi_j^{(m)}(x,z,t), \tag{A45}$$

where $\phi_j^{(m)}(x,z,t)$ is as the format of $\phi(x,z,t)$ in Eq. (A43) and can be induced by $v_j^{(m)}$ in Fig. 10 in proportion.

When the induced potential by the first finger of a unit in all the periods reads

$$\phi_0(x,z,t) = \sum_{m=1}^{M} \phi_0^{(m)}(x,z,t), \tag{A46}$$

then the potential induced by the other two fingers in a period reads

$$\begin{aligned}\phi_1(x,z,t) &= \phi_0(x-2p',z,t) \\ &= \sum_{m=1}^{M} \phi_0^{(m)}\left(x-\frac{\lambda}{3},z,t\right), \\ \phi_2(x,z,t) &= \phi_0\left(x-4p',z,t\right) \\ &= \sum_{m=1}^{M} \phi_0^{(m)}\left(x-\frac{2\lambda}{3},z,t\right).\end{aligned} \tag{A47}$$

Assume the applied voltage on the jth electrode in a period is $V_j = v_j^{(1)} = v_j^{(2)} = \cdots = v_j^{(M)}$ in Fig. 10 with $j = 0, 1, 2$, then the overall acquired potential is

$$\begin{aligned}V(x,z,t) &= \sum_{j=0}^{2} V_j v_j(x,z,t) \\ &= V_0 \sum_{m=1}^{M} \phi_0^{(m)}(x,z,t) + V_1 \sum_{m=1}^{M} \phi_0^{(m)}\left(x-\frac{\lambda}{3},z,t\right) \\ &\quad + V_2 \sum_{m=1}^{M} \phi_0^{(m)}\left(x-\frac{2\lambda}{3},z,t\right),\end{aligned} \tag{A48}$$

where $\phi_0^{(m)}(x,z,t) = \Re[B_0 e^{-kz} e^{ik(x-vt)}]$ with B_0 representing the amplitude of the potential at $z = 0$.

Then the induced electric field vector $\vec{E}(x,z,t)$ by $V(x,z,t)$ is

$$\vec{E}(x,z,t) = -\nabla V(x,z,t) = [E_x, E_z]^T, \tag{A49}$$

where

$$\begin{aligned}E_x &= -V_0 \frac{\partial \sum_{m=1}^{M} v_0^{(m)}(x,z)}{\partial x} - V_1 \frac{\sum_{m=1}^{M} v_0^{(m)}\left(x-\frac{\lambda}{3},z\right)}{\partial x} \\ &\quad - V_2 \frac{\partial \sum_{m=1}^{M} v_0^{(m)}\left(x-\frac{2\lambda}{3},z\right)}{\partial x}, \\ E_z &= -V_0 \frac{\partial \sum_{m=1}^{M} \Re\left[B_0 e^{-kz} e^{ik(x-vt)}\right]}{\partial z} \\ &\quad - V_1 \frac{\partial \sum_{m=1}^{M} \Re\left[B_0 e^{-kz} e^{ik\left(x-\frac{\lambda}{3}-vt\right)}\right]}{\partial z} \\ &\quad - V_2 \frac{\partial \sum_{m=1}^{M} \Re\left[B_0 e^{-kz} e^{ik\left(x-\frac{2\lambda}{3}-vt\right)}\right]}{\partial z}.\end{aligned} \tag{A50}$$

For the passive receiving IDT in Fig. 10, $V_0 = V_1 \neq V_2$, the above electric field can be simplified as

$$\begin{aligned}E_x &= M(V_0 - V_2) B_0 k e^{-kz} \sin\left[k\left(x-\frac{2\lambda}{3}-vt\right)\right], \\ E_z &= M(V_2 - V_0) B_0 k e^{-kz} \cos\left[k\left(x-\frac{2\lambda}{3}-vt\right)\right].\end{aligned} \tag{A51}$$

APPENDIX B: SIMPLIFYING THE INTERACTION BETWEEN POLAR MOLECULE AND ELECTRIC FIELD BY SAW WITH ROTATING WAVE APPROXIMATION

Here we introduce in detail the method to simplify the dependence on the time-varying components in the Hamiltonian in Eq. (3) via rotating wave approximation. We firstly define a transformed quantum state ket $|\psi'(t)\rangle$ based on the original ket $|\tilde{\psi}(t)\rangle$, then we have [57,58]

$$i\hbar \frac{d}{dt}|\tilde{\psi}(t)\rangle = H|\tilde{\psi}(t)\rangle, \tag{B1a}$$

$$|\psi'(t)\rangle = e^{i\mathbf{A}t}|\tilde{\psi}(t)\rangle, \tag{B1b}$$

$$i\hbar \frac{d}{dt}|\psi'(t)\rangle = H_\omega|\psi'(t)\rangle, \tag{B1c}$$

where $\hbar = 1$ for simplification and $\mathbf{U} = e^{i\mathbf{A}t}$ represents the transformation between $|\tilde{\psi}(t)\rangle$ and $|\psi'(t)\rangle$, H in Eq. (B1a)

is given in Eq. (3), and in Eq. (B1c)

$$\begin{aligned} H_\omega &= e^{i\mathbf{A}t}(H-\mathbf{A})e^{-i\mathbf{A}t} \\ &= e^{i\mathbf{A}t}\begin{bmatrix} \omega_1 - kv/2 & -|\vec{\mu}|E_z^{(j)}(x,z,t)\frac{m\Omega}{J'(J'+1)} \\ -|\vec{\mu}|E_z^{(j)}(x,z,t)\frac{m\Omega}{J'(J'+1)} & \omega_2 + kv/2 \end{bmatrix} e^{-i\mathbf{A}t} \\ &= \begin{bmatrix} \bar{\omega} + \frac{\bar{E}_\Delta - kv}{2} & -\frac{|\vec{\mu}|m\Omega}{J'(J'+1)}E_z^{(j)}(x,z,t)e^{ikvt} \\ -\frac{|\vec{\mu}|m\Omega}{J'(J'+1)}E_z^{(j)}(x,z,t)e^{-ikvt} & \bar{\omega} - \frac{\bar{E}_\Delta - kv}{2} \end{bmatrix}, \end{aligned} \tag{B2}$$

where $\mathbf{A} = \left[\begin{smallmatrix} kv/2 & 0 \\ 0 & -kv/2 \end{smallmatrix}\right]$, $\bar{\omega} = (\omega_1+\omega_2)/2$, and the time-varying component can be simplified as

$$\begin{aligned} -|\vec{\mu}|\frac{m\Omega}{J'(J'+1)}E_z^{(j)}(x,z,t)e^{-ikvt} &= (-1)^j\frac{|\vec{\mu}|m\Omega M\bar{u}_j k}{J'(J'+1)}e^{-k\tilde{z}_j} \\ \frac{e^{i[k(x-\frac{2\lambda}{3}-vt)]} + e^{-i[k(x-\frac{2\lambda}{3}-vt)]}}{2}e^{-ikvt} &\approx (-1)^j\frac{|\vec{\mu}|m\Omega M\bar{u}_j k}{2J'(J'+1)}e^{-k\tilde{z}_j}e^{-ik(x-\frac{2\lambda}{3})}, \end{aligned} \tag{B3}$$

by neglecting the fast oscillating terms containing e^{-2ikvt}. Then we have Eq. (4) in the main text.

APPENDIX C: ILLUSTRATION ON EQ. (9)

During the trapping of polar molecules, the motion of molecules is determined by the electric force and Newtonian mechanics. In the longitudinal direction, the molecules can be stable because the direction of the joint force by the IDT-induced electric field and the external electric force are different at the upper side and the lower side of the trapped points and this can provide the restoring force. In the horizontal direction, once the polar molecules can escape from the trapped localization, their motion is only determined by the IDT-induced electric field as Eq. (7) in the main text. Consider the property of the electric force at a point only affected by the IDT but not by the external force, which satisfies that

$$\begin{aligned} &\vec{\nabla}\cdot\vec{F}(x,z,t) \\ &= -\vec{\nabla}\cdot\left(\frac{1}{2}\frac{1}{|\vec{E}|}\frac{dU}{d|\vec{E}|}\vec{\nabla}|\vec{E}|^2\right) \\ &= -\frac{1}{2}\vec{\nabla}\cdot\left\{\frac{1}{|\vec{E}|}\frac{dU}{d|\vec{E}|}\vec{\nabla}\left[\left(\frac{\partial\phi}{\partial x}\right)^2+\left(\frac{\partial\phi}{\partial z}\right)^2\right]\right\} \\ &= -\vec{\nabla}\cdot\left\{\frac{1}{|\vec{E}|}\frac{dU}{d|\vec{E}|}\left[\left(\frac{\partial\phi}{\partial x}\frac{\partial^2\phi}{\partial x^2}+\frac{\partial\phi}{\partial z}\frac{\partial^2\phi}{\partial z\partial x}\right)\vec{x}+\left(\frac{\partial\phi}{\partial x}\frac{\partial^2\phi}{\partial x\partial z}+\frac{\partial\phi}{\partial z}\frac{\partial^2\phi}{\partial z^2}\right)\vec{z}\right]\right\} \\ &= -\frac{1}{|\vec{E}|}\frac{dU}{d|\vec{E}|}\left[\left(\frac{\partial^2\phi}{\partial x^2}\frac{\partial^2\phi}{\partial x^2}+\frac{\partial\phi}{\partial x}\frac{\partial^3\phi}{\partial x^3}+\frac{\partial^2\phi}{\partial z\partial x}\frac{\partial^2\phi}{\partial z\partial x}+\frac{\partial\phi}{\partial z}\frac{\partial^3\phi}{\partial z\partial x^2}\right)+\left(\frac{\partial^2\phi}{\partial x\partial z}\frac{\partial^2\phi}{\partial x\partial z}+\frac{\partial\phi}{\partial x}\frac{\partial^3\phi}{\partial x\partial z^2}-\frac{\partial^2\phi}{\partial z^2}\frac{\partial^2\phi}{\partial x^2}-\frac{\partial\phi}{\partial z}\frac{\partial^3\phi}{\partial^2 x\partial z}\right)\right] \\ &= -\frac{1}{|\vec{E}|}\frac{dU}{d|\vec{E}|}\left[\left(\frac{\partial^2\phi}{\partial x^2}\right)^2+\left(\frac{\partial^2\phi}{\partial z^2}\right)^2+\frac{\partial\phi}{\partial x}\left(\frac{\partial^3\phi}{\partial x^3}+\frac{\partial^3\phi}{\partial x\partial z^2}\right)+\frac{\partial\phi}{\partial z}\left(\frac{\partial^3\phi}{\partial z\partial x^2}-\frac{\partial^3\phi}{\partial x^2\partial z}\right)+2\left(\frac{\partial^2\phi}{\partial z\partial x}\right)^2\right] \\ &= -\frac{1}{|\vec{E}|}\frac{dU}{d|\vec{E}|}\left[\left(\frac{\partial^2\phi}{\partial x^2}\right)^2+\left(\frac{\partial^2\phi}{\partial z^2}\right)^2+2\left(\frac{\partial^2\phi}{\partial z\partial x}\right)^2\right] \\ &= -\frac{\mu_{\text{eff}}^2}{\sqrt{\left(\frac{E_\Delta}{2}\right)^2+\left(\mu_{\text{eff}}|\vec{E}|\right)^2}}\left[\left(\frac{\partial^2\phi}{\partial x^2}\right)^2+\left(\frac{\partial^2\phi}{\partial z^2}\right)^2+2\left(\frac{\partial^2\phi}{\partial z\partial x}\right)^2\right] < 0, \end{aligned} \tag{C1}$$

where $\phi = \phi(x,z,t)$ is given in Eq. (A43) [59,102].

[1] L. D. Carr, D. DeMille, R. V. Krems, and J. Ye, Cold and ultracold molecules: Science, technology and applications, New J. Phys. **11**, 055049 (2009).

[2] K. Mishima and K. Yamashita, Quantum computing using rotational modes of two polar molecules, Chem. Phys. **361**, 106 (2009).

[3] D. DeMille, Quantum computation with trapped polar molecules, Phys. Rev. Lett. **88**, 067901 (2002).

[4] R. Sawant, J. A. Blackmore, P. D. Gregory, J. Mur-Petit, D. Jaksch, J. Aldegunde, J. M. Hutson, M. Tarbutt, and S. L. Cornish, Ultracold polar molecules as qudits, New J. Phys. **22**, 013027 (2020).

[5] A. André, D. DeMille, J. M. Doyle, M. D. Lukin, S. E. Maxwell, P. Rabl, R. J. Schoelkopf, and P. Zoller, A coherent all-electrical interface between polar molecules and mesoscopic superconducting resonators, Nat. Phys. **2**, 636 (2006).

[6] S. F. Yelin, K. Kirby, and R. Côté, Schemes for robust quantum computation with polar molecules, Phys. Rev. A **74**, 050301(R) (2006).

[7] C. P. Koch, M. Lemeshko, and D. Sugny, Quantum control of molecular rotation, Rev. Mod. Phys. **91**, 035005 (2019).

[8] M. Ortner, A. Micheli, G. Pupillo, and P. Zoller, Quantum simulations of extended Hubbard models with dipolar crystals, New J. Phys. **11**, 055045 (2009).

[9] I. M. Georgescu, S. Ashhab, and F. Nori, Quantum simulation, Rev. Mod. Phys. **86**, 153 (2014).

[10] R. J. Bartlett and M. Musiał, Coupled-cluster theory in quantum chemistry, Rev. Mod. Phys. **79**, 291 (2007).

[11] J. Doyle, B. Friedrich, R. Krems, and F. Masnou-Seeuws, Quo vadis, cold molecules? Eur. Phys. J. D **31**, 149 (2004).

[12] J. D. Weinstein, R. DeCarvalho, T. Guillet, B. Friedrich, and J. M. Doyle, Magnetic trapping of calcium monohydride molecules at millikelvin temperatures, Nature (London) **395**, 148 (1998).

[13] B. C. Sawyer, B. L. Lev, E. R. Hudson, B. K. Stuhl, M. Lara, J. L. Bohn, and J. Ye, Magnetoelectrostatic trapping of ground state oh molecules, Phys. Rev. Lett. **98**, 253002 (2007).

[14] D. J. McCarron, M. H. Steinecker, Y. Zhu, and D. DeMille, Magnetic trapping of an ultracold gas of polar molecules, Phys. Rev. Lett. **121**, 013202 (2018).

[15] L. Caldwell and M. R. Tarbutt, General approach to state-dependent optical-tweezer traps for polar molecules, Phys. Rev. Res. **3**, 013291 (2021).

[16] J. T. Zhang, Y. Yu, W. B. Cairncross, K. Wang, L. R. B. Picard, J. D. Hood, Y.-W. Lin, J. M. Hutson, and K.-K. Ni, Forming a single molecule by magnetoassociation in an optical tweezer, Phys. Rev. Lett. **124**, 253401 (2020).

[17] L. R. Liu, J. D. Hood, Y. Yu, J. T. Zhang, K. Wang, Y.-W. Lin, T. Rosenband, and K.-K. Ni, Molecular assembly of ground-state cooled single atoms, Phys. Rev. X **9**, 021039 (2019).

[18] L. Liu, J. Hood, Y. Yu, J. Zhang, N. Hutzler, T. Rosenband, and K.-K. Ni, Building one molecule from a reservoir of two atoms, Science **360**, 900 (2018).

[19] B. Friedrich, Electro-optical trap for polar molecules, Phys. Rev. A **105**, 053126 (2022).

[20] S. A. Meek, H. Conrad, and G. Meijer, Trapping molecules on a chip, Science **324**, 1699 (2009).

[21] H. Guo, Y. Ji, Q. Liu, T. Yang, S. Hou, and J. Yin, Controllable three-dimensional electrostatic lattices for manipulation of cold polar molecules, Phys. Rev. A **105**, 053108 (2022).

[22] S. Y. T. van de Meerakker, P. H. M. Smeets, N. Vanhaecke, R. T. Jongma, and G. Meijer, Deceleration and electrostatic trapping of OH radicals, Phys. Rev. Lett. **94**, 023004 (2005).

[23] T. Rieger, T. Junglen, S. A. Rangwala, P. W. H. Pinkse, and G. Rempe, Continuous loading of an electrostatic trap for polar molecules, Phys. Rev. Lett. **95**, 173002 (2005).

[24] R. Blümel, Electrodynamic trap for neutral polar particles, Phys. Rev. A **83**, 045402 (2011).

[25] J. van Veldhoven, H. L. Bethlem, and G. Meijer, Ac electric trap for ground-state molecules, Phys. Rev. Lett. **94**, 083001 (2005).

[26] H. L. Bethlem, F. M. H. Crompvoets, R. T. Jongma, S. Y. T. van de Meerakker, and G. Meijer, Deceleration and trapping of ammonia using time-varying electric fields, Phys. Rev. A **65**, 053416 (2002).

[27] M. Tarbutt, J. Hudson, B. Sauer, and E. Hinds, Prospects for measuring the electric dipole moment of the electron using electrically trapped polar molecules, Faraday Discuss. **142**, 37 (2009).

[28] E. Charron, P. Milman, A. Keller, and O. Atabek, Quantum phase gate and controlled entanglement with polar molecules, Phys. Rev. A **75**, 033414 (2007).

[29] T. Rom, T. Best, O. Mandel, A. Widera, M. Greiner, T. W. Hänsch, and I. Bloch, State selective production of molecules in optical lattices, Phys. Rev. Lett. **93**, 073002 (2004).

[30] A. Micheli, G. K. Brennen, and P. Zoller, A toolbox for lattice-spin models with polar molecules, Nat. Phys. **2**, 341 (2006).

[31] D. Mitra, K. H. Leung, and T. Zelevinsky, Quantum control of molecules for fundamental physics, Phys. Rev. A **105**, 040101 (2022).

[32] K. Hermansson and H. Tepper, Electric field effects on vibrating polar molecules from weak to strong fields, Mol. Phys. **89**, 1291 (1996).

[33] R. M. Hochstrasser, Electric field effects on oriented molecules and molecular crystals, Acc. Chem. Res. **6**, 263 (1973).

[34] E. R. Hudson, Experiments on cold molecules produced via stark deceleration, Ph.D. thesis, University of Colorado at Boulder, 2006

[35] E. R. Hudson, J. Bochinski, H. Lewandowski, B. C. Sawyer, and J. Ye, Efficient stark deceleration of cold polar molecules, Eur. Phys. J. D **31**, 351 (2004).

[36] S. A. Meek, A stark decelerator on a chip, Ph.D. thesis, Fritz-Haber-Institut der Max-Planck-Gesellschaft, Germany, 2010.

[37] G. J. Simpson, V. García-López, A. Daniel Boese, J. M. Tour, and L. Grill, How to control single-molecule rotation, Nat. Commun. **10**, 4631 (2019).

[38] E. R. Hudson, Deceleration of continuous molecular beams, Phys. Rev. A **79**, 061407(R) (2009).

[39] B. C. Sawyer, B. K. Stuhl, B. L. Lev, J. Ye, and E. R. Hudson, Mitigation of loss within a molecular stark decelerator, Eur. Phys. J. D **48**, 197 (2008).

[40] D. Morgan, *Surface Acoustic Wave Filters: With Applications to Electronic Communications and Signal Processing* (Academic Press, Boca Raton, FL, 2010).

[41] K.-y. Hashimoto and K.-Y. Hashimoto, *Surface Acoustic Wave Devices in Telecommunications* (Springer, New York, 2000), Vol. 116.

[42] J. P. Robinson, M. P. Kennett, N. R. Cooper, and V. I. Fal'ko, Surface acoustic-wave-induced magnetoresistance oscillations in a two-dimensional electron gas, Phys. Rev. Lett. **93**, 036804 (2004).

[43] T. Byrnes, P. Recher, N. Y. Kim, S. Utsunomiya, and Y. Yamamoto, Quantum simulator for the Hubbard model with long-range coulomb interactions using surface acoustic waves, Phys. Rev. Lett. **99**, 016405 (2007).

[44] L. Tracy, J. Eisenstein, M. Lilly, L. Pfeiffer, and K. West, Surface acoustic wave propagation and inhomogeneities in low-density two-dimensional electron systems near the metal–insulator transition, Solid State Commun. **137**, 150 (2006).

[45] S. H. Simon, Coupling of surface acoustic waves to a two-dimensional electron gas, Phys. Rev. B **54**, 13878 (1996).

[46] M. J. A. Schuetz, J. Knoerzer, G. Giedke, L. M. K. Vandersypen, M. D. Lukin, and J. I. Cirac, Acoustic traps and lattices for electrons in semiconductors, Phys. Rev. X **7**, 041019 (2017).

[47] S. A. Moses, J. P. Covey, M. T. Miecnikowski, D. S. Jin, and J. Ye, New frontiers for quantum gases of polar molecules, Nat. Phys. **13**, 13 (2017).

[48] K.-K. Ni, S. Ospelkaus, D. Wang, G. Quéméner, B. Neyenhuis, M. De Miranda, J. Bohn, J. Ye, and D. Jin, Dipolar collisions of polar molecules in the quantum regime, Nature (London) **464**, 1324 (2010).

[49] Z. Chen, L. Li, W. Shi, and H. Guo, Optimization design of a Lamb wave device for density sensing of nonviscous liquid, IEEE Trans. Ultrason., Ferroelect., Freq. Contr. **54**, 1949 (2007).

[50] A. Jhunjhunwala and J. Vetelino, Spectrum of acoustic waves emanating from an IDT on a piezoelectric half space, in *1979 Ultrasonics Symposium* (IEEE, Piscataway, NJ, 1979), pp. 945–950.

[51] G. Gumbs, G. R. Aĭzin, and M. Pepper, Interaction of surface acoustic waves with a narrow electron channel in a piezoelectric material, Phys. Rev. B **57**, 1654 (1998).

[52] S. A. Meek, H. L. Bethlem, H. Conrad, and G. Meijer, Trapping molecules on a chip in traveling potential wells, Phys. Rev. Lett. **100**, 153003 (2008).

[53] A. N. Bolgar, J. I. Zotova, D. D. Kirichenko, I. S. Besedin, A. V. Semenov, R. S. Shaikhaidarov, and O. V. Astafiev, Quantum regime of a two-dimensional phonon cavity, Phys. Rev. Lett. **120**, 223603 (2018).

[54] H. Guo, Y. Ji, Q. Liu, T. Yang, S. Hou, and J. Yin, A driven three-dimensional electric lattice for polar molecules, Front. Phys. **17**, 52505 (2022).

[55] G. Chen, H. Zhang, Y. Yang, R. Wang, L. Xiao, and S. Jia, Qubit-induced high-order nonlinear interaction of the polar molecules in a stripline cavity, Phys. Rev. A **82**, 013601 (2010).

[56] S. A. Meek, H. Conrad, and G. Meijer, A stark decelerator on a chip, New J. Phys. **11**, 055024 (2009).

[57] M. Hughes, M. D. Frye, R. Sawant, G. Bhole, J. A. Jones, S. L. Cornish, M. R. Tarbutt, J. M. Hutson, D. Jaksch, and J. Mur-Petit, Robust entangling gate for polar molecules using magnetic and microwave fields, Phys. Rev. A **101**, 062308 (2020).

[58] C.-Y. Tai, R. T. Deck, and C. Kim, ac-Stark-effect-enhanced four-wave mixing in a near-resonant four-level system, Phys. Rev. A **37**, 163 (1988).

[59] K. Wohlfart, F. Filsinger, F. Grätz, J. Küpper, and G. Meijer, Stark deceleration of oh radicals in low-field-seeking and high-field-seeking quantum states, Phys. Rev. A **78**, 033421 (2008).

[60] H. L. Bethlem, M. R. Tarbutt, J. Küpper, D. Carty, K. Wohlfart, E. Hinds, and G. Meijer, Alternating gradient focusing and deceleration of polar molecules, J. Phys. B **39**, R263 (2006).

[61] H. L. Bethlem, J. van Veldhoven, M. Schnell, and G. Meijer, Trapping polar molecules in an ac trap, Phys. Rev. A **74**, 063403 (2006).

[62] D.-W. Wang, M. D. Lukin, and E. Demler, Quantum fluids of self-assembled chains of polar molecules, Phys. Rev. Lett. **97**, 180413 (2006).

[63] M. Klawunn, A. Pikovski, and L. Santos, Two-dimensional scattering and bound states of polar molecules in bilayers, Phys. Rev. A **82**, 044701 (2010).

[64] P. W. Anderson, Absence of diffusion in certain random lattices, Phys. Rev. **109**, 1492 (1958).

[65] T. Xu and R. V. Krems, Quantum walk and Anderson localization of rotational excitations in disordered ensembles of polar molecules, New J. Phys. **17**, 065014 (2015).

[66] G. L. Celardo, R. Kaiser, and F. Borgonovi, Shielding and localization in the presence of long-range hopping, Phys. Rev. B **94**, 144206 (2016).

[67] L. F. Santos, F. Borgonovi, and G. L. Celardo, Cooperative shielding in many-body systems with long-range interaction, Phys. Rev. Lett. **116**, 250402 (2016).

[68] J. T. Cantin, T. Xu, and R. V. Krems, Effect of the anisotropy of long-range hopping on localization in three-dimensional lattices, Phys. Rev. B **98**, 014204 (2018).

[69] L. Pollet, S. M. A. Rombouts, and P. J. H. Denteneer, Ultracold atoms in one-dimensional optical lattices approaching the Tonks-Girardeau regime, Phys. Rev. Lett. **93**, 210401 (2004).

[70] K. Biedron, M. Lacki, and J. Zakrzewski, Extended Bose-Hubbard model with dipolar and contact interactions, Phys. Rev. B **97**, 245102 (2018).

[71] D. Jaksch, C. Bruder, J. I. Cirac, C. W. Gardiner, and P. Zoller, Cold bosonic atoms in optical lattices, Phys. Rev. Lett. **81**, 3108 (1998).

[72] C. A. Stafford and S. Das Sarma, Collective Coulomb blockade in an array of quantum dots: A Mott-Hubbard approach, Phys. Rev. Lett. **72**, 3590 (1994).

[73] P. Buonsante and A. Vezzani, Ground-state fidelity and bipartite entanglement in the Bose-Hubbard model, Phys. Rev. Lett. **98**, 110601 (2007).

[74] T. Sowiński, O. Dutta, P. Hauke, L. Tagliacozzo, and M. Lewenstein, Dipolar molecules in optical lattices, Phys. Rev. Lett. **108**, 115301 (2012).

[75] M. Klinsmann, D. Peter, and H. P. Büchler, Ferroelectric quantum phase transition with cold polar molecules, New J. Phys. **17**, 085002 (2015).

[76] B. Damski, L. Santos, E. Tiemann, M. Lewenstein, S. Kotochigova, P. Julienne, and P. Zoller, Creation of a dipolar superfluid in optical lattices, Phys. Rev. Lett. **90**, 110401 (2003).

[77] I. Bloch, J. Dalibard, and W. Zwerger, Many-body physics with ultracold gases, Rev. Mod. Phys. **80**, 885 (2008).

[78] U. Bissbort, F. Deuretzbacher, and W. Hofstetter, Effective multibody-induced tunneling and interactions in the Bose-Hubbard model of the lowest dressed band of an optical lattice, Phys. Rev. A **86**, 023617 (2012).

[79] O. Dutta, A. Eckardt, P. Hauke, B. Malomed, and M. Lewenstein, Bose–Hubbard model with occupation-dependent parameters, New J. Phys. **13**, 023019 (2011).

[80] O. Dutta, M. Gajda, P. Hauke, M. Lewenstein, D.-S. Lühmann, B. A. Malomed, T. Sowiński, and J. Zakrzewski, Non-standard Hubbard models in optical lattices: A review, Rep. Prog. Phys. **78**, 066001 (2015).

[81] J. K. Freericks and H. Monien, Strong-coupling expansions for the pure and disordered Bose-Hubbard model, Phys. Rev. B **53**, 2691 (1996).

[82] M. P. A. Fisher, P. B. Weichman, G. Grinstein, and D. S. Fisher, Boson localization and the superfluid-insulator transition, Phys. Rev. B **40**, 546 (1989).

[83] L. Amico and V. Penna, Dynamical mean field theory of the Bose-Hubbard model, Phys. Rev. Lett. **80**, 2189 (1998).

[84] J. Freericks and H. Monien, Phase diagram of the Bose-Hubbard model, Europhys. Lett. **26**, 545 (1994).

[85] T. D. Kühner and H. Monien, Phases of the one-dimensional Bose-Hubbard model, Phys. Rev. B **58**, R14741 (1998).

[86] I. Stasyuk and T. Mysakovych, Phase diagrams of the Bose-Hubbard model at finite temperature, Condens. Matter Phys. **12**, 539 (2009).

[87] G. Mahan, Lattice gas theory of ionic conductivity, Phys. Rev. B **14**, 780 (1976).

[88] I. Stasyuk and I. Dulepa, Density of states of one-dimensional Pauli ionic conductor, Condens. Matter Phys. **10**, 259 (2007).

[89] M. Quintero-Pérez, P. Jansen, T. E. Wall, J. E. van den Berg, S. Hoekstra, and H. L. Bethlem, Static trapping of polar molecules in a traveling wave decelerator, Phys. Rev. Lett. **110**, 133003 (2013).

[90] T. Volz, N. Syassen, D. M. Bauer, E. Hansis, S. Dürr, and G. Rempe, Preparation of a quantum state with one molecule at each site of an optical lattice, Nat. Phys. **2**, 692 (2006).

[91] Z. Meng, L. Wang, W. Han, F. Liu, K. Wen, C. Gao, P. Wang, C. Chin, and J. Zhang, Atomic Bose–Einstein condensate in twisted-bilayer optical lattices, Nature (London) **615**, 231 (2023).

[92] B. Capogrosso-Sansone, C. Trefzger, M. Lewenstein, P. Zoller, and G. Pupillo, Quantum phases of cold polar molecules in 2D optical lattices, Phys. Rev. Lett. **104**, 125301 (2010).

[93] D.-W. Wang, Quantum phase transitions of polar molecules in bilayer systems, Phys. Rev. Lett. **98**, 060403 (2007).

[94] M. Greiner, O. Mandel, T. Esslinger, T. W. Hänsch, and I. Bloch, Quantum phase transition from a superfluid to a Mott insulator in a gas of ultracold atoms, Nature (London) **415**, 39 (2002).

[95] K. R. A. Hazzard, B. Gadway, M. Foss-Feig, B. Yan, S. A. Moses, J. P. Covey, N. Y. Yao, M. D. Lukin, J. Ye, D. S. Jin, and A. M. Rey, Many-body dynamics of dipolar molecules in an optical lattice, Phys. Rev. Lett. **113**, 195302 (2014).

[96] C. T. Hann, C.-L. Zou, Y. Zhang, Y. Chu, R. J. Schoelkopf, S. M. Girvin, and L. Jiang, Hardware-efficient quantum random access memory with hybrid quantum acoustic systems, Phys. Rev. Lett. **123**, 250501 (2019).

[97] R. Stoneley, The propagation of surface elastic waves in a cubic crystal, Proc. R. Soc. London A **232**, 447 (1955).

[98] M. J. A. Schuetz, E. M. Kessler, G. Giedke, L. M. K. Vandersypen, M. D. Lukin, and J. I. Cirac, Universal quantum transducers based on surface acoustic waves, Phys. Rev. X **5**, 031031 (2015).

[99] S. Hou, B. Wei, L. Deng, and J. Yin, Chip-based microtrap arrays for cold polar molecules, Phys. Rev. A **96**, 063416 (2017).

[100] Z.-X. Lin, S. Wu, R. Ro, and M.-S. Lee, Surface acoustic wave properties of (100) AlN films on diamond with different IDT positions, IEEE Trans. Ultrason. Ferroelectr. Freq. Control **56**, 1246 (2009).

[101] M. B. Mazalan, A. M. Noor, Y. Wahab, S. Yahud, and W. S. W. K. Zaman, Current development in interdigital transducer (IDT) surface acoustic wave devices for live cell in vitro studies: A review, Micromachines **13**, 30 (2021).

[102] G. R. Aĭzin, G. Gumbs, and M. Pepper, Screening of the surface-acoustic-wave potential by a metal gate and the quantization of the acoustoelectric current in a narrow channel, Phys. Rev. B **58**, 10589 (1998).